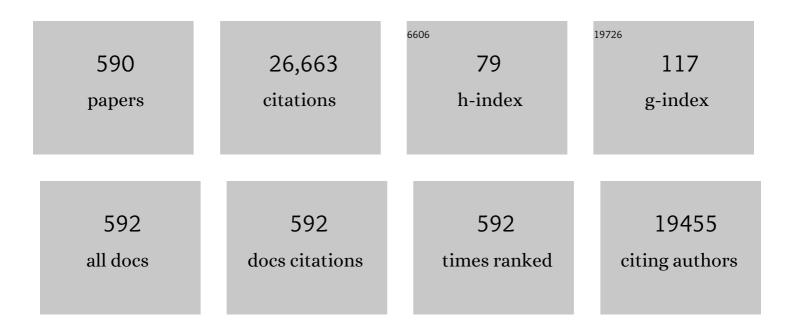


List of Publications by Year in descending order

Source: https://exaly.com/author-pdf/3848826/publications.pdf Version: 2024-02-01



#	Article	IF	CITATIONS
1	Boosted Electrocatalytic N ₂ Reduction to NH ₃ by Defectâ€Rich MoS ₂ Nanoflower. Advanced Energy Materials, 2018, 8, 1801357.	10.2	482
2	Synthesis of amino functionalized magnetic graphenes composite material and its application to remove Cr(VI), Pb(II), Hg(II), Cd(II) and Ni(II) from contaminated water. Journal of Hazardous Materials, 2014, 278, 211-220.	6.5	469
3	Highly efficient removal of heavy metal ions by amine-functionalized mesoporous Fe3O4 nanoparticles. Chemical Engineering Journal, 2012, 184, 132-140.	6.6	324
4	Adsorption of phosphate from aqueous solution by hydroxy-aluminum, hydroxy-iron and hydroxy-iron–aluminum pillared bentonites. Journal of Hazardous Materials, 2010, 179, 244-250.	6.5	306
5	A critical review on antibiotics and hormones in swine wastewater: Water pollution problems and control approaches. Journal of Hazardous Materials, 2020, 387, 121682.	6.5	295
6	Co(OH) ₂ Nanoparticleâ€Encapsulating Conductive Nanowires Array: Roomâ€Temperature Electrochemical Preparation for Highâ€Performance Water Oxidation Electrocatalysis. Advanced Materials, 2018, 30, 1705366.	11.1	294
7	High-Performance N ₂ -to-NH ₃ Conversion Electrocatalyzed by Mo ₂ C Nanorod. ACS Central Science, 2019, 5, 116-121.	5.3	292
8	Electrochemical N ₂ fixation to NH ₃ under ambient conditions: Mo ₂ N nanorod as a highly efficient and selective catalyst. Chemical Communications, 2018, 54, 8474-8477.	2.2	287
9	Label-free photoelectrochemical immunoassay for CEA detection based on CdS sensitized WO3@BiOI heterostructure nanocomposite. Biosensors and Bioelectronics, 2018, 99, 493-499.	5.3	206
10	Electrochemical bisphenol A sensor based on N-doped graphene sheets. Analytica Chimica Acta, 2012, 711, 24-28.	2.6	200
11	Ag3PO4/graphene-oxide composite with remarkably enhanced visible-light-driven photocatalytic activity toward dyes in water. Journal of Hazardous Materials, 2013, 244-245, 86-93.	6.5	200
12	Self-Luminescent Lanthanide Metal–Organic Frameworks as Signal Probes in Electrochemiluminescence Immunoassay. Journal of the American Chemical Society, 2021, 143, 504-512.	6.6	195
13	Label-free immunosensor for the detection of kanamycin using Ag@Fe3O4 nanoparticles and thionine mixed graphene sheet. Biosensors and Bioelectronics, 2013, 48, 224-229.	5.3	181
14	Removal of mercury and methylene blue from aqueous solution by xanthate functionalized magnetic graphene oxide: Sorption kinetic and uptake mechanism. Journal of Colloid and Interface Science, 2015, 439, 112-120.	5.0	173
15	Extracellular polymeric substances for Zn (II) binding during its sorption process onto aerobic granular sludge. Journal of Hazardous Materials, 2016, 301, 407-415.	6.5	161
16	Cathodic electrochemiluminescence immunosensor based on nanocomposites of semiconductor carboxylated g-C3N4 and graphene for the ultrasensitive detection of squamous cell carcinoma antigen. Biosensors and Bioelectronics, 2014, 55, 330-336.	5.3	158
17	Self-supported CoMoS4 nanosheet array as an efficient catalyst for hydrogen evolution reaction at neutral pH. Nano Research, 2018, 11, 2024-2033.	5.8	147
18	A critical review on membrane hybrid system for nutrient recovery from wastewater. Chemical Engineering Journal, 2018, 348, 143-156.	6.6	145

#	Article	IF	CITATIONS
19	A MoS ₂ nanosheet–reduced graphene oxide hybrid: an efficient electrocatalyst for electrocatalytic N ₂ reduction to NH ₃ under ambient conditions. Journal of Materials Chemistry A, 2019, 7, 2524-2528.	5.2	145
20	Sulfur-Doped Graphene-Based Immunological Biosensing Platform for Multianalysis of Cancer Biomarkers. ACS Applied Materials & Interfaces, 2017, 9, 37637-37644.	4.0	144
21	Removal of Pb(II) and methylene blue from aqueous solution by magnetic hydroxyapatite-immobilized oxidized multi-walled carbon nanotubes. Journal of Colloid and Interface Science, 2017, 494, 380-388.	5.0	140
22	Electrochemical ultrasensitive detection of cardiac troponin I using covalent organic frameworks for signal amplification. Biosensors and Bioelectronics, 2018, 119, 176-181.	5.3	138
23	Label-free electrochemical immunosensor based on flower-like Ag/MoS2/rGO nanocomposites for ultrasensitive detection of carcinoembryonic antigen. Sensors and Actuators B: Chemical, 2018, 255, 125-132.	4.0	135
24	Dual-Quenching Electrochemiluminescence Strategy Based on Three-Dimensional Metal–Organic Frameworks for Ultrasensitive Detection of Amyloid-β. Analytical Chemistry, 2019, 91, 1989-1996.	3.2	135
25	A silver–palladium alloy nanoparticle-based electrochemical biosensor for simultaneous detection of ractopamine, clenbuterol and salbutamol. Biosensors and Bioelectronics, 2013, 49, 14-19.	5.3	134
26	3D Nanostructured Palladium-Functionalized Graphene-Aerogel-Supported Fe ₃ O ₄ for Enhanced Ru(bpy) ₃ ²⁺ -Based Electrochemiluminescent Immunosensing of Prostate Specific Antigen. ACS Applied Materials & Interfaces, 2017, 9, 35260-35267.	4.0	130
27	Nanobody-Based Apolipoprotein E Immunosensor for Point-of-Care Testing. ACS Sensors, 2017, 2, 1267-1271.	4.0	130
28	Label-free photoelectrochemical aptasensor for tetracycline detection based on cerium doped CdS sensitized BiYWO6. Biosensors and Bioelectronics, 2018, 106, 7-13.	5.3	129
29	A novel sandwich-type electrochemical immunosensor for PSA detection based on PtCu bimetallic hybrid (2D/2D) rGO/g-C3N4. Biosensors and Bioelectronics, 2017, 91, 441-448.	5.3	128
30	Using reduced graphene oxide-Ca:CdSe nanocomposite to enhance photoelectrochemical activity of gold nanoparticles functionalized tungsten oxide for highly sensitive prostate specific antigen detection. Biosensors and Bioelectronics, 2017, 96, 239-245.	5.3	128
31	Sensitive Electrochemical Sensor for Simultaneous Determination of Dopamine, Ascorbic Acid, and Uric Acid Enhanced by Amino-group Functionalized Mesoporous Fe3O4@Graphene Sheets. Electrochimica Acta, 2014, 116, 244-249.	2.6	127
32	Electrochemiluminescence immunosensor based on quenching effect of SiO2@PDA on SnO2/rGO/Au NPs-luminol for insulin detection. Sensors and Actuators B: Chemical, 2018, 265, 403-411.	4.0	127
33	Electrochemical immunosensors for cancer biomarker with signal amplification based on ferrocene functionalized iron oxide nanoparticles. Biosensors and Bioelectronics, 2011, 26, 3590-3595.	5.3	126
34	An amorphous FeMoS ₄ nanorod array toward efficient hydrogen evolution electrocatalysis under neutral conditions. Chemical Communications, 2017, 53, 9000-9003.	2.2	124
35	Dual Intramolecular Electron Transfer for In Situ Coreactantâ€Embedded Electrochemiluminescence Microimaging of Membrane Protein. Angewandte Chemie - International Edition, 2021, 60, 197-201.	7.2	121
36	Cobalt–borate nanowire array as a high-performance catalyst for oxygen evolution reaction in near-neutral media. Journal of Materials Chemistry A, 2017, 5, 7291-7294.	5.2	120

#	Article	IF	CITATIONS
37	Fe-doped Ni2P nanosheets with porous structure for electroreduction of nitrogen to ammonia under ambient conditions. Applied Catalysis B: Environmental, 2020, 263, 118296.	10.8	120
38	The removal of lead ions from aqueous solution by using magnetic hydroxypropyl chitosan/oxidized multiwalled carbon nanotubes composites. Journal of Colloid and Interface Science, 2015, 451, 7-14.	5.0	118
39	Efficient Enhancement of Electrochemiluminescence from Cadmium Sulfide Quantum Dots by Glucose Oxidase Mimicking Gold Nanoparticles for Highly Sensitive Assay of Methyltransferase Activity. Analytical Chemistry, 2016, 88, 2976-2983.	3.2	118
40	A novel label-free electrochemical immunosensor based on graphene and thionine nanocomposite. Sensors and Actuators B: Chemical, 2010, 149, 314-318.	4.0	117
41	Ultrasensitive electrochemical immunoassay for CEA through host–guest interaction of β-cyclodextrin functionalized graphene and Cu@Ag core–shell nanoparticles with adamantine-modified antibody. Biosensors and Bioelectronics, 2015, 63, 465-471.	5.3	117
42	Characterization of a multi-metal binding biosorbent: Chemical modification and desorption studies. Bioresource Technology, 2015, 193, 477-487.	4.8	116
43	Ultrasensitive electrochemical immunoassay for BRCA1 using BMIM·BF4-coated SBA-15 as labels and functionalized graphene as enhancer. Biomaterials, 2011, 32, 2117-2123.	5.7	115
44	Preparation and utilization of anaerobic granular sludge-based biochar for the adsorption of methylene blue from aqueous solutions. Journal of Molecular Liquids, 2014, 198, 334-340.	2.3	112
45	Ultrasensitive detection of kanamycin in animal derived foods by label-free electrochemical immunosensor. Food Chemistry, 2012, 134, 1601-1606.	4.2	111
46	EDTA modified β-cyclodextrin/chitosan for rapid removal of Pb(II) and acid red from aqueous solution. Journal of Colloid and Interface Science, 2018, 523, 56-64.	5.0	111
47	Phosphorylated chitosan/CoFe2O4 composite for the efficient removal of Pb(II) and Cd(II) from aqueous solution: Adsorption performance and mechanism studies. Journal of Molecular Liquids, 2019, 277, 181-188.	2.3	109
48	A novel ECL biosensor for the detection of concanavalin A based on glucose functionalized NiCo 2 S 4 nanoparticles-grown on carboxylic graphene as quenching probe. Biosensors and Bioelectronics, 2017, 96, 113-120.	5.3	107
49	Nanoporous PtRu Alloy Enhanced Nonenzymatic Immunosensor for Ultrasensitive Detection of Microcystin‣R. Advanced Functional Materials, 2011, 21, 4193-4198.	7.8	103
50	Macroporous graphene capped Fe3O4 for amplified electrochemiluminescence immunosensing of carcinoembryonic antigen detection based on CeO2@TiO2. Biosensors and Bioelectronics, 2017, 91, 842-848.	5.3	103
51	Ultrasensitive amperometric immunosensor for PSA detection based on Cu2O@CeO2-Au nanocomposites as integrated triple signal amplification strategy. Biosensors and Bioelectronics, 2017, 87, 630-637.	5.3	102
52	Visible-light driven label-free photoelectrochemical immunosensor based on TiO2/S-BiVO4@Ag2S nanocomposites for sensitive detection OTA. Biosensors and Bioelectronics, 2018, 99, 14-20.	5.3	102
53	Simultaneous nitrification-denitrification and membrane fouling alleviation in a submerged biofilm membrane bioreactor with coupling of sponge and biodegradable PBS carrier. Bioresource Technology, 2018, 270, 156-165.	4.8	102
54	Increased electrocatalyzed performance through high content potassium doped graphene matrix and aptamer tri infinite amplification labels strategy: Highly sensitive for matrix metalloproteinases-2 detection. Biosensors and Bioelectronics, 2017, 94, 694-700.	5.3	101

#	Article	IF	CITATIONS
55	Label-free electrochemical immunosensor for prostate-specific antigen based on silver hybridized mesoporous silica nanoparticles. Analytical Biochemistry, 2013, 434, 123-127.	1.1	100
56	A sensitive electrochemiluminescence immunosensor based on Ru(bpy) 3 2+ in 3D CuNi oxalate as luminophores and graphene oxide–polyethylenimine as released Ru(bpy) 3 2+ initiator. Biosensors and Bioelectronics, 2017, 89, 1020-1025.	5.3	100
57	CoC ₂ O ₄ ·2H ₂ O derived Co ₃ O ₄ nanorods array: a high-efficiency 1D electrocatalyst for alkaline oxygen evolution reaction. Chemical Communications, 2018, 54, 1533-1536.	2.2	99
58	An electrochemical aptasensor based on gold-modified MoS2/rGO nanocomposite and gold-palladium-modified Fe-MOFs for sensitive detection of lead ions. Sensors and Actuators B: Chemical, 2020, 319, 128313.	4.0	99
59	Mechanism of Pb(<scp>ii</scp>) and methylene blue adsorption onto magnetic carbonate hydroxyapatite/graphene oxide. RSC Advances, 2015, 5, 9759-9770.	1.7	98
60	Synthesis of Self-Supported Amorphous CoMoO ₄ Nanowire Array for Highly Efficient Hydrogen Evolution Reaction. ACS Sustainable Chemistry and Engineering, 2017, 5, 10093-10098.	3.2	98
61	Nanoporous gold film based immunosensor for label-free detection of cancer biomarker. Biosensors and Bioelectronics, 2011, 26, 3714-3718.	5.3	97
62	Label-Free Electrochemiluminescent Immunosensor for Detection of Carcinoembryonic Antigen Based on Nanocomposites of GO/MWCNTs-COOH/Au@CeO ₂ . ACS Applied Materials & Interfaces, 2015, 7, 19260-19267.	4.0	97
63	Electrochemiluminescent immunosensing of prostate-specific antigen based on silver nanoparticles-doped Pb (II) metal-organic framework. Biosensors and Bioelectronics, 2016, 79, 379-385.	5.3	97
64	Visible light photoelectrochemical aptasensor for adenosine detection based on CdS/PPy/g-C3N4 nanocomposites. Biosensors and Bioelectronics, 2016, 86, 439-445.	5.3	96
65	Dumbbell-like Au-Fe3O4 nanoparticles as label for the preparation of electrochemical immunosensors. Biosensors and Bioelectronics, 2010, 26, 627-631.	5.3	94
66	A prostate-specific antigen electrochemical immunosensor based on Pd NPs functionalized electroactive Co-MOF signal amplification strategy. Biosensors and Bioelectronics, 2019, 132, 97-104.	5.3	93
67	Label-free immunosensor based on Pd nanoplates for amperometric immunoassay of alpha-fetoprotein. Biosensors and Bioelectronics, 2014, 53, 305-309.	5.3	90
68	Label-free Electrochemiluminescent Immunosensor for Detection of Prostate Specific Antigen based on Aminated Graphene Quantum Dots and Carboxyl Graphene Quantum Dots. Scientific Reports, 2016, 6, 20511.	1.6	89
69	Enzyme-free electrochemical immunosensor configured with Au–Pd nanocrystals and N-doped graphene sheets for sensitive detection of AFP. Biosensors and Bioelectronics, 2013, 49, 222-225.	5.3	88
70	The role of nanomaterials in electroanalytical biosensors: A mini review. Journal of Electroanalytical Chemistry, 2016, 781, 401-409.	1.9	88
71	Sandwich-type electrochemical immunosensor for CEA detection based on Ag/MoS2@Fe3O4 and an an analogous ELISA method with total internal reflection microscopy. Sensors and Actuators B: Chemical, 2018, 266, 561-569.	4.0	88
72	<i>In situ</i> electrochemical development of copper oxide nanocatalysts within a TCNQ nanowire array: a highly conductive electrocatalyst for the oxygen evolution reaction. Chemical Communications, 2018, 54, 1425-1428.	2.2	88

#	Article	IF	CITATIONS
73	Sensitive Insulin Detection based on Electrogenerated Chemiluminescence Resonance Energy Transfer between Ru(bpy) ₃ ²⁺ and Au Nanoparticle-Doped β-Cyclodextrin-Pb (II) Metal–Organic Framework. ACS Applied Materials & Interfaces, 2016, 8, 10121-10127.	4.0	87
74	Synthesis of amino-functionalized magnetic aerobic granular sludge-biochar for Pb(II) removal: Adsorption performance and mechanism studies. Science of the Total Environment, 2019, 685, 681-689.	3.9	87
75	Facile fabrication of an aptasensor for thrombin based on graphitic carbon nitride/TiO2 with high visible-light photoelectrochemical activity. Biosensors and Bioelectronics, 2016, 75, 116-122.	5.3	86
76	Electrochemical aptasensor based on gold modified thiol graphene as sensing platform and gold-palladium modified zirconium metal-organic frameworks nanozyme as signal enhancer for ultrasensitive detection of mercury ions. Journal of Colloid and Interface Science, 2022, 606, 510-517.	5.0	86
77	Electrochemiluminescent competitive immunosensor based on polyethyleneimine capped SiO2 nanomaterials as labels to release Ru(bpy)32+ fixed in 3D Cu/Ni oxalate for the detection of aflatoxin B1. Biosensors and Bioelectronics, 2018, 101, 290-296.	5.3	85
78	An ultrasensitive sandwich-type electrochemical immunosensor based on signal amplification strategy of gold nanoparticles functionalized magnetic multi-walled carbon nanotubes loaded with lead ions. Biosensors and Bioelectronics, 2015, 68, 626-632.	5.3	83
79	Magnetic chitosan/anaerobic granular sludge composite: Synthesis, characterization and application in heavy metal ions removal. Journal of Colloid and Interface Science, 2017, 508, 405-414.	5.0	83
80	Smart Drug Delivery System-Inspired Enzyme-Linked Immunosorbent Assay Based on Fluorescence Resonance Energy Transfer and Allochroic Effect Induced Dual-Modal Colorimetric and Fluorescent Detection. Analytical Chemistry, 2018, 90, 1976-1982.	3.2	79
81	Efficient electrohydrogenation of N ₂ to NH ₃ by oxidized carbon nanotubes under ambient conditions. Chemical Communications, 2019, 55, 4997-5000.	2.2	79
82	Construction of self-powered cytosensing device based on ZnO nanodisks@g-C3N4 quantum dots and application in the detection of CCRF-CEM cells. Nano Energy, 2018, 46, 101-109.	8.2	78
83	Label-free amperometric immunosensor for the detection of human serum chorionic gonadotropin based on nanoporous gold and graphene. Analytical Biochemistry, 2011, 414, 196-201.	1.1	77
84	Role of extracellular polymeric substances in biosorption of dye wastewater using aerobic granular sludge. Bioresource Technology, 2015, 185, 14-20.	4.8	77
85	Ultrasensitive photoelectrochemical immunosensor for the detection of amyloid β-protein based on SnO2/SnS2/Ag2S nanocomposites. Biosensors and Bioelectronics, 2018, 120, 1-7.	5.3	77
86	Graphene-Based Optical and Electrochemical Biosensors: A Review. Analytical Letters, 2013, 46, 1-17.	1.0	76
87	Ultra-thin wrinkled NiOOH–NiCr ₂ O ₄ nanosheets on Ni foam: an advanced catalytic electrode for oxygen evolution reaction. Chemical Communications, 2018, 54, 4987-4990.	2.2	76
88	Oxygen defect engineering in cobalt iron oxide nanosheets for promoted overall water splitting. Journal of Materials Chemistry A, 2019, 7, 21704-21710.	5.2	76
89	Ferritin-Based Electrochemiluminescence Nanosurface Energy Transfer System for Procalcitonin Detection Using HWRGWVC Heptapeptide for Site-Oriented Antibody Immobilization. Analytical Chemistry, 2019, 91, 7145-7152.	3.2	76
90	Simultaneous electrochemical detection of cervical cancer markers using reduced graphene oxide-tetraethylene pentamine as electrode materials and distinguishable redox probes as labels. Biosensors and Bioelectronics, 2014, 54, 634-639.	5.3	75

#	Article	IF	CITATIONS
91	A sandwich-type electrochemical immunosensor based on multiple signal amplification for α-fetoprotein labeled by platinum hybrid multiwalled carbon nanotubes adhered copper oxide. Electrochimica Acta, 2015, 160, 7-14.	2.6	75
92	Eco-friendly synthesis of electrochemiluminescent nitrogen-doped carbon quantum dots from diethylene triamine pentacetate and their application for protein detection. Carbon, 2015, 91, 144-152.	5.4	75
93	A novel label-free photoelectrochemical sensor based on N,S-GQDs and CdS co-sensitized hierarchical Zn2SnO4 cube for detection of cardiac troponin I. Biosensors and Bioelectronics, 2018, 106, 14-20.	5.3	75
94	Quenching Electrochemiluminescence Immunosensor Based on Resonance Energy Transfer between Ruthenium (II) Complex Incorporated in the UiO-67 Metal–Organic Framework and Gold Nanoparticles for Insulin Detection. ACS Applied Materials & Interfaces, 2018, 10, 22932-22938.	4.0	75
95	Fe3O4 nanoparticles-loaded PEG–PLA polymeric vesicles as labels for ultrasensitive immunosensors. Biomaterials, 2010, 31, 7332-7339.	5.7	74
96	Removal of Hg(II) from aqueous solution by resin loaded magnetic β-cyclodextrin bead and graphene oxide sheet: Synthesis, adsorption mechanism and separation properties. Journal of Colloid and Interface Science, 2015, 456, 42-49.	5.0	74
97	Sandwich-type electrochemical immunoassay based on Co3O4@MnO2-thionine and pseudo-ELISA method toward sensitive detection of alpha fetoprotein. Biosensors and Bioelectronics, 2018, 106, 179-185.	5.3	74
98	Label-free photoelectrochemical immunosensor for sensitive detection of Ochratoxin A. Biosensors and Bioelectronics, 2015, 64, 13-18.	5.3	73
99	Ultrasensitive electrochemical immunosensor for carbohydrate antigen 72-4 based on dual signal amplification strategy of nanoporous gold and polyaniline–Au asymmetric multicomponent nanoparticles. Biosensors and Bioelectronics, 2015, 64, 51-56.	5.3	73
100	Ultrasensitive electrochemical immunosensor for SCCA detection based on ternary Pt/PdCu nanocube anchored on three-dimensional graphene framework for signal amplification. Biosensors and Bioelectronics, 2016, 79, 71-78.	5.3	73
101	Facile fabrication of 3D flower-like heterostructured g-C ₃ N ₄ /SnS ₂ composite with efficient photocatalytic activity under visible light. RSC Advances, 2014, 4, 31019-31027.	1.7	71
102	Toxicity assessment of 4-chlorophenol to aerobic granular sludge and its interaction with extracellular polymeric substances. Journal of Hazardous Materials, 2015, 289, 101-107.	6.5	71
103	A label-free photoelectrochemical aptasensing platform base on plasmon Au coupling with MOF-derived In2O3@g-C3N4 nanoarchitectures for tetracycline detection. Sensors and Actuators B: Chemical, 2019, 298, 126817.	4.0	71
104	Synthesis and Application of CeO ₂ /SnS ₂ Heterostructures as a Highly Efficient Coreaction Accelerator in the Luminol–Dissolved O ₂ System for Ultrasensitive Biomarkers Immunoassay. Analytical Chemistry, 2019, 91, 14066-14073.	3.2	71
105	Electrochemical aptasensor based on gold modified graphene nanocomposite with different morphologies for ultrasensitive detection of Pb2+. Sensors and Actuators B: Chemical, 2019, 288, 325-331.	4.0	71
106	Dual-responsive electrochemical immunosensor for prostate specific antigen detection based on Au-CoS/graphene and CeO2/ionic liquids doped with carboxymethyl chitosan complex. Biosensors and Bioelectronics, 2017, 94, 141-147.	5.3	70
107	Ultrasensitive electrochemical immunosensor for quantitative detection of HBeAg using Au@Pd/MoS2@MWCNTs nanocomposite as enzyme-mimetic labels. Biosensors and Bioelectronics, 2018, 102, 189-195.	5.3	70
108	Biological denitrification in an anoxic sequencing batch biofilm reactor: Performance evaluation, nitrous oxide emission and microbial community. Bioresource Technology, 2019, 285, 121359.	4.8	70

#	Article	IF	CITATIONS
109	A label-free electrochemical immunosensor based on Au@Pd/Ag yolk-bimetallic shell nanoparticles and amination graphene for detection of nuclear matrix protein 22. Sensors and Actuators B: Chemical, 2014, 202, 67-73.	4.0	69
110	Photoelectrochemical sensitive detection of insulin based on CdS/polydopamine co-sensitized WO 3 nanorod and signal amplification of carbon nanotubes@polydopamine. Biosensors and Bioelectronics, 2017, 96, 345-350.	5.3	69
111	Electrochemical immunosensor for norethisterone based on signal amplification strategy of graphene sheets and multienzyme functionalized mesoporous silica nanoparticles. Biosensors and Bioelectronics, 2010, 26, 723-729.	5.3	68
112	CuS as co-reaction accelerator in PTCA-K2S2O8 system for enhancing electrochemiluminescence behavior of PTCA and its application in detection of amyloid-β protein. Biosensors and Bioelectronics, 2019, 126, 222-229.	5.3	68
113	A photoelectrochemical sensor for highly sensitive detection of amyloid beta based on sensitization of Mn:CdSe to Bi2WO6/CdS. Biosensors and Bioelectronics, 2018, 122, 37-42.	5.3	67
114	High-performance N ₂ -to-NH ₃ fixation by a metal-free electrocatalyst. Nanoscale, 2019, 11, 4231-4235.	2.8	67
115	Ultrasensitive electrochemical immunosensors for multiplexed determination using mesoporous platinum nanoparticles as nonenzymatic labels. Analytica Chimica Acta, 2014, 807, 44-50.	2.6	66
116	A label-free amperometric immunosensor for detection of zearalenone based on trimetallic Au-core/AgPt-shell nanorattles and mesoporous carbon. Analytica Chimica Acta, 2014, 847, 29-36.	2.6	66
117	Metal ions-based immunosensor for simultaneous determination of estradiol and diethylstilbestrol. Biosensors and Bioelectronics, 2014, 52, 225-231.	5.3	66
118	Facile synthesis of MoS2@Cu2O-Pt nanohybrid as enzyme-mimetic label for the detection of the Hepatitis B surface antigen. Biosensors and Bioelectronics, 2018, 100, 512-518.	5.3	66
119	Guiding protein delivery into live cells using DNA-programmed membrane fusion. Chemical Science, 2018, 9, 5967-5975.	3.7	66
120	Immobilization of glucose oxidase and platinum on mesoporous silica nanoparticles for the fabrication of glucose biosensor. Electrochimica Acta, 2011, 56, 2960-2965.	2.6	65
121	Sandwich-type electrochemical immunosensor for the detection of AFP based on Pd octahedral and APTES-M-CeO2-GS as signal labels. Biosensors and Bioelectronics, 2016, 79, 482-487.	5.3	65
122	An ultrasensitive photoelectrochemical immunosensor for insulin detection based on BiOBr/Ag 2 S composite by in-situ growth method with high visible-light activity. Biosensors and Bioelectronics, 2017, 97, 253-259.	5.3	65
123	Bioactivity-Protected Electrochemiluminescence Biosensor Using Gold Nanoclusters as the Low-Potential Luminophor and Cu ₂ S Snowflake as Co-reaction Accelerator for Procalcitonin Analysis. ACS Sensors, 2019, 4, 1909-1916.	4.0	65
124	Quench-Type Electrochemiluminescence Immunosensor Based on Resonance Energy Transfer from Carbon Nanotubes and Au-Nanoparticles-Enhanced <i>g</i> -C ₃ N ₄ to CuO@Polydopamine for Procalcitonin Detection. ACS Applied Materials & Interfaces, 2020, 12, 8006-8015.	4.0	65
125	A "turn-off―fluorescent biosensor for the detection of mercury (II) based on graphite carbon nitride. Talanta, 2017, 162, 46-51.	2.9	64
126	Amorphous Co-doped MoO _x nanospheres with a core–shell structure toward an effective oxygen evolution reaction. Journal of Materials Chemistry A, 2019, 7, 1005-1012.	5.2	64

#	Article	IF	CITATIONS
127	Self-Supply of H ₂ O ₂ and O ₂ by Hydrolyzing CaO ₂ to Enhance the Electrochemiluminescence of Luminol Based on a Closed Bipolar Electrode. Analytical Chemistry, 2020, 92, 12693-12699.	3.2	64
128	Corallite-like Magnetic Fe ₃ O ₄ @MnO ₂ @Pt Nanocomposites as Multiple Signal Amplifiers for the Detection of Carcinoembryonic Antigen. ACS Applied Materials & Interfaces, 2015, 7, 18786-18793.	4.0	63
129	Highly selective fluorescent chemosensor for detection of Fe3+ based on Fe3O4@ZnO. Scientific Reports, 2016, 6, 23558.	1.6	63
130	Facile synthesis of cuprous oxide nanowires decorated graphene oxide nanosheets nanocomposites and its application in label-free electrochemical immunosensor. Biosensors and Bioelectronics, 2017, 87, 745-751.	5.3	63
131	Phase-junction design of MOF-derived TiO2 photoanodes sensitized with quantum dots for efficient hydrogen generation. Applied Catalysis B: Environmental, 2020, 263, 118317.	10.8	63
132	Ultrasensitive sandwich-type electrochemical immunosensor based on a novel signal amplification strategy using highly loaded toluidine blue/gold nanoparticles decorated KIT-6/carboxymethyl chitosan/ionic liquids as signal labels. Biosensors and Bioelectronics, 2014, 61, 618-624.	5.3	62
133	A novel electrochemiluminescent immunosensor based on the quenching effect of aminated graphene on nitrogen-doped carbon quantum dots. Analytica Chimica Acta, 2015, 889, 82-89.	2.6	62
134	Nitrogen removal via nitrite in a partial nitrification sequencing batch biofilm reactor treating high strength ammonia wastewater and its greenhouse gas emission. Bioresource Technology, 2017, 230, 49-55.	4.8	62
135	Sensitive sandwich electrochemical immunosensor for alpha fetoprotein based on prussian blue modified hydroxyapatite. Biosensors and Bioelectronics, 2011, 28, 112-116.	5.3	61
136	Application of Europium Multiwalled Carbon Nanotubes as Novel Luminophores in an Electrochemiluminescent Aptasensor for Thrombin Using Multiple Amplification Strategies. ACS Applied Materials & Interfaces, 2015, 7, 12663-12670.	4.0	61
137	Comparative study of the role of extracellular polymeric substances in biosorption of Ni(II) onto aerobic/anaerobic granular sludge. Journal of Colloid and Interface Science, 2017, 490, 754-761.	5.0	61
138	Ultrasensitive electrochemical immunoassay for squamous cell carcinoma antigen using dumbbell-like Pt–Fe3O4 nanoparticles as signal amplification. Biosensors and Bioelectronics, 2013, 46, 91-96.	5.3	60
139	Plasmon enhanced photoelectrochemical sensing of mercury (II) ions in human serum based on Au@Ag nanorods modified TiO2 nanosheets film. Biosensors and Bioelectronics, 2016, 79, 866-873.	5.3	60
140	Ratiometric electrochemical immunosensor for the detection of procalcitonin based on the ratios of SiO2-Fc–COOH–Au and UiO-66-TB complexes. Biosensors and Bioelectronics, 2021, 171, 112713.	5.3	60
141	A bio-chemical application of N-GQDs and g-C3N4 QDs sensitized TiO2 nanopillars for the quantitative detection of pcDNA3-HBV. Biosensors and Bioelectronics, 2017, 91, 456-464.	5.3	59
142	System performance and microbial community succession in a partial nitrification biofilm reactor in response to salinity stress. Bioresource Technology, 2018, 270, 512-518.	4.8	59
143	Label-free photoelectrochemical immunosensor for NT-proBNP detection based on La-CdS/3D ZnIn2S4/Au@ZnO sensitization structure. Biosensors and Bioelectronics, 2018, 117, 773-780.	5.3	59
144	Ultrasensitive non-enzymatic immunosensor for carcino-embryonic antigen based on palladium hybrid vanadium pentoxide/multiwalled carbon nanotubes. Biosensors and Bioelectronics, 2016, 77, 1104-1111.	5.3	58

#	Article	IF	CITATIONS
145	Bioinspired synthesis of organic–inorganic hybrid nanoflowers for robust enzyme-free electrochemical immunoassay. Biosensors and Bioelectronics, 2019, 133, 94-99.	5.3	58
146	Ultrasensitive near-infrared electrochemiluminescence biosensor derived from Eu-MOF with antenna effect and high efficiency catalysis of specific CoS2 hollow triple shelled nanoboxes for procalcitonin. Biosensors and Bioelectronics, 2021, 191, 113409.	5.3	58
147	Ultrasensitive electrochemical aptasensor for the detection of thrombin based on dual signal amplification strategy of Au@GS and DNA-CoPd NPs conjugates. Biosensors and Bioelectronics, 2016, 80, 640-646.	5.3	57
148	Ni(OH)2/NGQDs-based electrochemiluminescence immunosensor for prostate specific antigen detection by coupling resonance energy transfer with Fe3O4@MnO2 composites. Biosensors and Bioelectronics, 2018, 99, 346-352.	5.3	57
149	Nitrogen removal in a combined aerobic granular sludge and solid-phase biological denitrification system: System evaluation and community structure. Bioresource Technology, 2019, 288, 121504.	4.8	57
150	Ultrasensitive Controlled Release Aptasensor Using Thymine–Hg ²⁺ –Thymine Mismatch as a Molecular Switch for Hg ²⁺ Detection. Analytical Chemistry, 2020, 92, 14069-14075.	3.2	57
151	An electrochemical immunosensor for ultrasensitive detection of carbohydrate antigen 199 based on Au@Cu x OS yolk–shell nanostructures with porous shells as labels. Biosensors and Bioelectronics, 2015, 63, 39-46.	5.3	56
152	Fabrication of In2S3/Zn2GeO4 composite photocatalyst for degradation of acetaminophen under visible light. Journal of Colloid and Interface Science, 2017, 506, 197-206.	5.0	56
153	Metal organic framework nanofibers derived Co3O4-doped carbon-nitrogen nanosheet arrays for high efficiency electrocatalytic oxygen evolution. Carbon, 2018, 137, 433-441.	5.4	56
154	A competitive photoelectrochemical immunosensor for the detection of diethylstilbestrol based on an Au/UiO-66(NH2)/CdS matrix and a direct Z-scheme Melem/CdTe heterojunction as labels. Biosensors and Bioelectronics, 2018, 117, 575-582.	5.3	56
155	A signal-off sandwich photoelectrochemical immunosensor using TiO2 coupled with CdS as the photoactive matrix and copper (II) ion as inhibitor. Biosensors and Bioelectronics, 2015, 65, 97-102.	5.3	55
156	A Compatible Sensitivity Enhancement Strategy for Electrochemiluminescence Immunosensors Based on the Biomimetic Melanin-Like Deposition. Analytical Chemistry, 2017, 89, 13049-13053.	3.2	55
157	Facile Synthesis of Cu ₂ O@TiO ₂ -PtCu Nanocomposites as a Signal Amplification Strategy for the Insulin Detection. ACS Applied Materials & Interfaces, 2019, 11, 8945-8953.	4.0	55
158	MnCO ₃ as a New Electrochemiluminescence Emitter for Ultrasensitive Bioanalysis of β-Amyloid _{1–42} Oligomers Based on Site-Directed Immobilization of Antibody. ACS Applied Materials & Interfaces, 2019, 11, 7157-7163.	4.0	54
159	Quench-type electrochemiluminescence immunosensor for detection of amyloid β-protein based on resonance energy transfer from luminol@SnS2-Pd to Cu doped WO3 nanoparticles. Biosensors and Bioelectronics, 2019, 133, 192-198.	5.3	54
160	Aggregation-Induced Electrochemiluminescence Bioconjugates of Apoferritin-Encapsulated Iridium(III) Complexes for Biosensing Application. Analytical Chemistry, 2021, 93, 1553-1560.	3.2	54
161	Effects of hydraulic retention time and bioflocculant addition on membrane fouling in a sponge-submerged membrane bioreactor. Bioresource Technology, 2016, 210, 11-17.	4.8	53
162	A sandwich-type photoelectrochemical immunosensor for NT-pro BNP detection based on F-Bi2WO6/Ag2S and GO/PDA for signal amplification. Biosensors and Bioelectronics, 2019, 131, 299-306.	5.3	53

#	Article	IF	CITATIONS
163	Novel signal amplification strategy for ultrasensitive sandwich-type electrochemical immunosensor employing Pd–Fe3O4-GS as the matrix and SiO2 as the label. Biosensors and Bioelectronics, 2015, 74, 59-65.	5.3	52
164	Ultrasensitive photoelectrochemical immunosensor of cardiac troponin I detection based on dual inhibition effect of Ag@Cu2O core-shell submicron-particles on CdS QDs sensitized TiO2 nanosheets. Biosensors and Bioelectronics, 2018, 117, 340-346.	5.3	52
165	Zinc-doping enhanced cadmium sulfide electrochemiluminescence behavior based on Au-Cu alloy nanocrystals quenching for insulin detection. Biosensors and Bioelectronics, 2017, 97, 115-121.	5.3	52
166	A visible light induced photoelectrochemical aptsensor constructed by aligned ZnO@CdTe core shell nanocable arrays/carboxylated g-C3N4 for the detection of Proprotein convertase subtilisin/kexin type 6 gene. Biosensors and Bioelectronics, 2015, 74, 49-58.	5.3	51
167	Anatase TiO ₂ based photoelectrochemical sensor for the sensitive determination of dopamine under visible light irradiation. New Journal of Chemistry, 2015, 39, 1483-1487.	1.4	51
168	Quenched electrochemiluminescence of Ag nanoparticles functionalized g-C3N4 by ferrocene for highly sensitive immunosensing. Analytica Chimica Acta, 2015, 854, 40-46.	2.6	51
169	Ultrasensitive competitive method-based electrochemiluminescence immunosensor for diethylstilbestrol detection based on Ru(bpy)32+ as luminophor encapsulated in metal–organic frameworks UiO-67. Biosensors and Bioelectronics, 2018, 110, 201-206.	5.3	51
170	Electrochemical immunosensor for ochratoxin A detection based on Au octahedron plasmonic colloidosomes. Analytica Chimica Acta, 2018, 1032, 114-121.	2.6	51
171	Application of anaerobic granular sludge for competitive biosorption of methylene blue and Pb(II): Fluorescence and response surface methodology. Bioresource Technology, 2015, 194, 297-304.	4.8	50
172	Label electrochemical immunosensor for prostate-specific antigen based on graphene and silver hybridized mesoporous silica. Analytical Biochemistry, 2015, 469, 76-82.	1.1	50
173	Graphene loaded bimetallic Au@Pt nanodendrites enhancing ultrasensitive electrochemical immunoassay of AFP. Sensors and Actuators B: Chemical, 2016, 231, 513-519.	4.0	50
174	Visible-light driven photoelectrochemical immunosensor for insulin detection based on MWCNTs@SnS2@CdS nanocomposites. Biosensors and Bioelectronics, 2016, 86, 301-307.	5.3	50
175	Sandwich-Type Electrochemiluminescence Sensor for Detection of NT-proBNP by Using High Efficiency Quench Strategy of Fe ₃ 0 ₄ @PDA toward Ru(bpy) ₃ ²⁺ Coordinated with Silver Oxalate. ACS Sensors, 2017, 2, 1774-1778.	4.0	50
176	Biosorption performance evaluation of heavy metal onto aerobic granular sludge-derived biochar in the presence of effluent organic matter via batch and fluorescence approaches. Bioresource Technology, 2018, 249, 410-416.	4.8	50
177	Performance, microbial community and fluorescent characteristic of microbial products in a solid-phase denitrification biofilm reactor for WWTP effluent treatment. Journal of Environmental Management, 2018, 227, 375-385.	3.8	50
178	Double electrochemiluminescence quenching effects of Fe3O4@PDA-CuXO towards self-enhanced Ru(bpy)32+ functionalized MOFs with hollow structure and it application to procalcitonin immunosensing. Biosensors and Bioelectronics, 2019, 142, 111521.	5.3	50
179	Label-free electrochemical immunosensor based on biocompatible nanoporous Fe ₃ O ₄ and biotin–streptavidin system for sensitive detection of zearalenone. Analyst, The, 2020, 145, 1368-1375.	1.7	50
180	Rare Self-Luminous Mixed-Valence Eu-MOF with a Self-Enhanced Characteristic as a Near-Infrared Fluorescent ECL Probe for Nondestructive Immunodetection. Analytical Chemistry, 2021, 93, 8613-8621.	3.2	50

#	Article	IF	CITATIONS
181	A label-free electrochemiluminescence immunosensor based on silver nanoparticle hybridized mesoporous carbon for the detection of Aflatoxin B1. Sensors and Actuators B: Chemical, 2014, 202, 53-59.	4.0	49
182	Nanosheet Au/Co3O4-based ultrasensitive nonenzymatic immunosensor for melanoma adhesion molecule antigen. Biosensors and Bioelectronics, 2014, 58, 345-350.	5.3	49
183	Partial nitrification granular sludge reactor as a pretreatment for anaerobic ammonium oxidation (Anammox): Achievement, performance and microbial community. Bioresource Technology, 2018, 269, 25-31.	4.8	49
184	Facile fabrication of an electrochemical aptasensor based on magnetic electrode by using streptavidin modified magnetic beads for sensitive and specific detection of Hg 2+. Biosensors and Bioelectronics, 2016, 82, 9-13.	5.3	48
185	Ultrasensitive Label-free Electrochemical Immunosensor based on Multifunctionalized Graphene Nanocomposites for the Detection of Alpha Fetoprotein. Scientific Reports, 2017, 7, 42361.	1.6	48
186	Ultrasensitive sandwich-type photoelectrochemical immunosensor based on CdSe sensitized La-TiO2 matrix and signal amplification of polystyrene@Ab2 composites. Biosensors and Bioelectronics, 2017, 87, 593-599.	5.3	48
187	Triple amplified ultrasensitive electrochemical immunosensor for alpha fetoprotein detection based on MoS2@Cu2O-Au nanoparticles. Sensors and Actuators B: Chemical, 2019, 297, 126821.	4.0	48
188	Fabrication of hierarchical MIL-68(In)-NH2/MWCNT/CdS composites for constructing label-free photoelectrochemical tetracycline aptasensor platform. Biosensors and Bioelectronics, 2019, 135, 88-94.	5.3	48
189	Photoelectrochemical Biosensor for Sensitive Detection of Soluble CD44 Based on the Facile Construction of a Poly(ethylene glycol)/Hyaluronic Acid Hybrid Antifouling Interface. ACS Applied Materials & Interfaces, 2019, 11, 24764-24770.	4.0	47
190	A dual-mode PCT electrochemical immunosensor with CuCo2S4 bimetallic sulfides as enhancer. Biosensors and Bioelectronics, 2020, 163, 112280.	5.3	47
191	Dual-Mode Electrochemical Immunoassay for Insulin Based on Cu ₇ S ₄ –Au as a Double Signal Indicator. ACS Applied Materials & Interfaces, 2018, 10, 38791-38798.	4.0	46
192	Boosting electrocatalytic nitrogen fixation <i>via</i> energy-efficient anodic oxidation of sodium gluconate. Chemical Communications, 2019, 55, 10170-10173.	2.2	46
193	"Greenâ€; gradient multi-shell CuInSe2/(CuInSexS1-x)5/CuInS2 quantum dots for photo-electrochemical hydrogen generation. Applied Catalysis B: Environmental, 2021, 280, 119402.	10.8	46
194	Defect-rich ZnS nanoparticles supported on reduced graphene oxide for high-efficiency ambient N2-to-NH3 conversion. Applied Catalysis B: Environmental, 2021, 284, 119746.	10.8	46
195	Ultrasensitive non-mediator electrochemical immunosensors using Au/Ag/Au core/double shell nanoparticles as enzyme-mimetic labels. Talanta, 2014, 124, 60-66.	2.9	45
196	Sandwich-type electrochemical immunosensor using dumbbell-like nanoparticles for the determination of gastric cancer biomarker CA72-4. Talanta, 2015, 134, 305-309.	2.9	45
197	Ultrasensitive photoelectrochemical aptasensing of miR-155 using efficient and stable CH3NH3PbI3 quantum dots sensitized ZnO nanosheets as light harvester. Biosensors and Bioelectronics, 2016, 85, 142-150.	5.3	44
198	Electrochemiluminescence Double Quenching System Based on Novel Emitter GdPO ₄ :Eu with Low-Excited Positive Potential for Ultrasensitive Procalcitonin Detection. ACS Sensors, 2019, 4, 2825-2831.	4.0	44

#	Article	IF	CITATIONS
199	Self-Powered Cathodic Photoelectrochemical Aptasensor Comprising a Photocathode and a Photoanode in Microfluidic Analysis Systems. Analytical Chemistry, 2021, 93, 7125-7132.	3.2	44
200	Ultrasensitive non-enzymatic and non-mediator electrochemical biosensor using nitrogen-doped graphene sheets for signal amplification and nanoporous alloy as carrier. Electrochimica Acta, 2013, 97, 105-111.	2.6	43
201	Ultrasensitive electrochemical immunosensor for zeranol detection based on signal amplification strategy of nanoporous gold films and nano-montmorillonite as labels. Analytica Chimica Acta, 2013, 758, 72-79.	2.6	43
202	lonic liquid functionalized graphene based immunosensor for sensitive detection of carbohydrate antigen 15-3 integrated with Cd2+-functionalized nanoporous TiO2 as labels. Biosensors and Bioelectronics, 2014, 59, 75-80.	5.3	43
203	Electrochemical immunosensor for α-fetoprotein detection using ferroferric oxide and horseradish peroxidase as signal amplification labels. Analytical Biochemistry, 2014, 465, 121-126.	1.1	43
204	Ultrasensitive sandwich-type electrochemical immunosensor based on dual signal amplification strategy using multifunctional graphene nanocomposites as labels for quantitative detection of tissue polypeptide antigen. Sensors and Actuators B: Chemical, 2015, 214, 124-131.	4.0	43
205	Ultrasensitive sandwich-type electrochemical immunosensor based on trimetallic nanocomposite signal amplification strategy for the ultrasensitive detection of CEA. Scientific Reports, 2016, 6, 30849.	1.6	43
206	A competitive-type photoelectrochemical immunosensor for aflatoxin B1 detection based on flower-like WO3 as matrix and Ag2S-enhanced BiVO4 for signal amplification. Sensors and Actuators B: Chemical, 2018, 270, 104-111.	4.0	43
207	A self-powered photoelectrochemical cathodic aptasensor for the detection of 17β-estradiol based on FeOOH/In2S3 photoanode. Biosensors and Bioelectronics, 2020, 154, 112089.	5.3	43
208	An ultrasensitive electrochemical immunosensor for the detection of salbutamol based on Pd@SBA-15 and ionic liquid. Electrochimica Acta, 2012, 69, 79-85.	2.6	42
209	A label-free electrochemiluminescence immunosensor based on KNbO3–Au nanoparticles@Bi2S3 for the detection of prostate specific antigen. Biosensors and Bioelectronics, 2015, 74, 104-112.	5.3	42
210	Ultrasensitive immunoassay for CA125 detection using acid site compound as signal and enhancer. Talanta, 2015, 144, 535-541.	2.9	42
211	Electrochemical DNA probe for Hg2+ detection based on a triple-helix DNA and Multistage Signal Amplification Strategy. Biosensors and Bioelectronics, 2016, 86, 907-912.	5.3	42
212	An electrochemical sensor based on Fe ₃ O ₄ @PANI nanocomposites for sensitive detection of Pb ²⁺ and Cd ²⁺ . Analytical Methods, 2018, 10, 4784-4792.	1.3	42
213	Cobalt-based metal-organic frameworks as co-reaction accelerator for enhancing electrochemiluminescence behavior of N-(aminobutyl)-N-(ethylisoluminol) and ultrasensitive immunosensing of amyloid-β protein. Sensors and Actuators B: Chemical, 2019, 291, 319-328.	4.0	42
214	Manganese doped CdS sensitized graphene/Cu2MoS4 composite for the photoelectrochemical immunoassay of cardiac troponin I. Biosensors and Bioelectronics, 2019, 132, 1-7.	5.3	42
215	Ultrasensitive amyloid-Î ² proteins detection based on curcumin conjugated ZnO nanoparticles quenching electrochemiluminescence behavior of luminol immobilized on Au@MoS2/Bi2S3 nanorods. Biosensors and Bioelectronics, 2019, 131, 136-142.	5.3	42
216	Electrochemiluminescent immunosensor for prostate specific antigen based upon luminol functionalized platinum nanoparticles loaded on graphene. Analytical Biochemistry, 2019, 566, 50-57.	1.1	42

#	Article	IF	CITATIONS
217	Oxygen Vacancy-Enhanced Electrochemiluminescence Sensing Strategy Using Luminol Thermally Encapsulated in Apoferritin as a Transducer for Biomarker Immunoassay. Analytical Chemistry, 2020, 92, 8472-8479.	3.2	42
218	Nonenzymatic immunosensor for detection of carbohydrate antigen 15-3 based on hierarchical nanoporous PtFe alloy. Biosensors and Bioelectronics, 2014, 56, 295-299.	5.3	41
219	Gold nanoparticles enhanced electrochemiluminescence of graphite-like carbon nitride for the detection of Nuclear Matrix Protein 22. Sensors and Actuators B: Chemical, 2014, 205, 176-183.	4.0	41
220	Electrochemical immunosensor for detecting typical bladder cancer biomarker based on reduced graphene oxide–tetraethylene pentamine and trimetallic AuPdPt nanoparticles. Talanta, 2015, 143, 77-82.	2.9	41
221	An ultrasensitive label-free immunosensor based on CdS sensitized Fe–TiO2 with high visible-light photoelectrochemical activity. Biosensors and Bioelectronics, 2015, 74, 843-848.	5.3	41
222	Photoelectrochemical Immunosensor for Detection of Carcinoembryonic Antigen Based on 2D TiO2 Nanosheets and Carboxylated Graphitic Carbon Nitride. Scientific Reports, 2016, 6, 27385.	1.6	41
223	Fabrication of magnetic water-soluble hyperbranched polyol functionalized graphene oxide for high-efficiency water remediation. Scientific Reports, 2016, 6, 28924.	1.6	41
224	Ultrasensitive immunosensor for prostate specific antigen using biomimetic polydopamine nanospheres as an electrochemiluminescence superquencher and antibody carriers. Analytica Chimica Acta, 2017, 963, 17-23.	2.6	41
225	Ultrasensitive electrochemical immunosensor for alpha fetoprotein detection based on platinum nanoparticles anchored on cobalt oxide/graphene nanosheets for signal amplification. Analytica Chimica Acta, 2017, 986, 138-144.	2.6	41
226	Rod-like Bi4O7 decorated Bi2O2CO3 plates: Facile synthesis, promoted charge separation, and highly efficient photocatalytic degradation of organic contaminants. Journal of Colloid and Interface Science, 2018, 514, 240-249.	5.0	41
227	Label-free photoelectrochemical immunosensor for carcinoembryonic antigen detection based on g-C3N4 nanosheets hybridized with Zn0.1Cd0.9S nanocrystals. Sensors and Actuators B: Chemical, 2018, 256, 812-819.	4.0	41
228	An ITO-based point-of-care colorimetric immunosensor for ochratoxin A detection. Talanta, 2018, 188, 593-599.	2.9	41
229	Ultrasensitive electrochemiluminescence immunosensor for the detection of amyloid-β proteins based on resonance energy transfer between g-C3N4 and Pd NPs coated NH2-MIL-53. Biosensors and Bioelectronics, 2019, 142, 111517.	5.3	41
230	Label-free electrochemical immunosensor for insulin detection by high-efficiency synergy strategy of Pd NPs@3D MoSx towards H2O2. Biosensors and Bioelectronics, 2019, 126, 108-114.	5.3	41
231	Nanobody-Based Electrochemical Immunoassay for Ultrasensitive Determination of Apolipoprotein-A1 Using Silver Nanoparticles Loaded Nanohydroxyapatite as Label. Analytical Chemistry, 2015, 87, 11209-11214.	3.2	40
232	A photoelectrochemical biosensor for fibroblast-like synoviocyte cell using visible light-activated NCQDs sensitized-ZnO/CH 3 NH 3 PbI 3 heterojunction. Biosensors and Bioelectronics, 2016, 77, 330-338.	5.3	40
233	Characterization of soluble microbial products in a partial nitrification sequencing batch biofilm reactor treating high ammonia nitrogen wastewater. Bioresource Technology, 2018, 249, 241-246.	4.8	40
234	Ultrasensitive Photoelectrochemical Biosensing Platform for Detecting N-Terminal Pro-brain Natriuretic Peptide Based on SnO ₂ /SnS ₂ /mpg-C ₃ N ₄ Amplified by PbS/SiO ₂ . ACS Applied Materials & Interfaces, 2018, 10, 31080-31087.	4.0	40

QIN WEI

#	Article	IF	CITATIONS
235	Dumbbell Plateâ€Shaped AlEgenâ€Based Luminescent MOF with High Quantum Yield as Selfâ€Enhanced ECL Tags: Mechanism Insights and Biosensing Application. Small, 2022, 18, e2106567.	5.2	40
236	Construction of label-free electrochemical immunosensor on mesoporous carbon nanospheres for breast cancer susceptibility gene. Analytica Chimica Acta, 2013, 770, 62-67.	2.6	39
237	A highly sensitive gas sensor based on Pd-doped Fe ₃ O ₄ nanoparticles for volatile organic compounds detection. Analytical Methods, 2014, 6, 886-892.	1.3	39
238	Cubic Cu 2 O nanoframes with a unique edge-truncated structure and a good electrocatalytic activity for immunosensor application. Biosensors and Bioelectronics, 2016, 78, 167-173.	5.3	39
239	Achievement, performance and characteristics of microbial products in a partial nitrification sequencing batch reactor as a pretreatment for anaerobic ammonium oxidation. Chemosphere, 2017, 183, 212-218.	4.2	39
240	Photoelectrochemical Cytosensing of RAW264.7 Macrophage Cells Based on a TiO ₂ Nanoneedls@MoO ₃ Array. Analytical Chemistry, 2017, 89, 7950-7957.	3.2	39
241	Enabling Electrocatalytic N ₂ Reduction to NH ₃ by Y ₂ O ₃ Nanosheet under Ambient Conditions. Industrial & Engineering Chemistry Research, 2018, 57, 16622-16627.	1.8	39
242	Sulfurâ€Ðoped CoO Nanoflakes with Loosely Packed Structure Realizing Enhanced Oxygen Evolution Reaction. Chemistry - A European Journal, 2018, 24, 17288-17292.	1.7	39
243	Using SiO2/PDA-Ag NPs to dual-inhibited photoelectrochemical activity of CeO2-CdS composites fabricated a novel immunosensor for BNP ultrasensitive detection. Sensors and Actuators B: Chemical, 2018, 274, 349-355.	4.0	39
244	A highly selective and sensitive detection of insulin withÂchemiluminescence biosensor based on aptamer and oligonucleotide-AuNPs functionalized nanosilica @ graphene oxide aerogel. Analytica Chimica Acta, 2019, 1089, 152-164.	2.6	39
245	Photoelectrochemical competitive immunosensor for 17β-estradiol detection based on ZnIn2S4@NH2-MIL-125(Ti) amplified by PDA NS/Mn:ZnCdS. Biosensors and Bioelectronics, 2020, 148, 111739.	5.3	39
246	Removal of Metanil Yellow from water environment by amino functionalized graphenes (NH2-G) – Influence of surface chemistry of NH2-G. Applied Surface Science, 2013, 284, 862-869.	3.1	38
247	Ultrasensitive nonenzymatic immunosensor based on bimetallic gold–silver nanoclusters synthesized by simple mortar grinding route. Sensors and Actuators B: Chemical, 2014, 194, 64-70.	4.0	38
248	Construction of dentate bonded TiO ₂ –CdSe heterostructures with enhanced photoelectrochemical properties: versatile labels toward photoelectrochemical and electrochemical sensing. Dalton Transactions, 2015, 44, 773-781.	1.6	38
249	Ultrasensitive photoelectrochemical immunosensor for insulin detection based on dual inhibition effect of CuS-SiO2 composite on CdS sensitized C-TiO2. Sensors and Actuators B: Chemical, 2018, 258, 1-9.	4.0	38
250	Assessment of microbial products in the biosorption process of Cu(II) onto aerobic granular sludge: Extracellular polymeric substances contribution and soluble microbial products release. Journal of Colloid and Interface Science, 2018, 527, 87-94.	5.0	38
251	Annihilation luminescent Eu-MOF as a near-infrared electrochemiluminescence probe for trace detection of trenbolone. Chemical Engineering Journal, 2022, 434, 134691.	6.6	38
252	Sensitive and selective determination of dopamine by electrochemical sensor based on molecularly imprinted electropolymerization of o-phenylenediamine. Analytical Methods, 2013, 5, 1469.	1.3	37

#	Article	IF	CITATIONS
253	Copper-doped titanium dioxide nanoparticles as dual-functional labels for fabrication of electrochemical immunosensors. Biosensors and Bioelectronics, 2014, 59, 335-341.	5.3	37
254	A generalized in situ electrodeposition of Zn doped CdS-based photoelectrochemical strategy for the detection of two metal ions on the same sensing platform. Biosensors and Bioelectronics, 2016, 77, 936-941.	5.3	37
255	Rapid removal of Pb(II) from aqueous solution using branched polyethylenimine enhanced magnetic carboxymethyl chitosan optimized with response surface methodology. Scientific Reports, 2017, 7, 10264.	1.6	37
256	Label-free ECL immunosensor for the early diagnosis of rheumatoid arthritis based on asymmetric heterogeneous polyaniline-gold nanomaterial. Sensors and Actuators B: Chemical, 2018, 257, 354-361.	4.0	37
257	A dual-signaling electrochemical ratiometric method for sensitive detection of carcinoembryonic antigen based on Au-Cu2S-CuS/graphene and Au-CeO2 supported toluidine blue complex. Sensors and Actuators B: Chemical, 2018, 256, 504-511.	4.0	37
258	Multivalent Aminosaccharide-Based Gold Nanoparticles as Narrow-Spectrum Antibiotics in Vivo. ACS Applied Materials & Interfaces, 2019, 11, 7725-7730.	4.0	37
259	Ni(OH)2 nanoarrays based molecularly imprinted polymer electrochemical sensor for sensitive detection of sulfapyridine. Sensors and Actuators B: Chemical, 2019, 287, 551-556.	4.0	37
260	Dual-signal electrochemiluminescence immunosensor for Neuron-specific enolase detection based on "dual-potential―emitter Ru(bpy)32+ functionalized zinc-based metal-organic frameworks. Biosensors and Bioelectronics, 2021, 192, 113505.	5.3	37
261	Sensitive electrochemical immunosensor for cancer biomarker with signal enhancement based on nitrodopamine-functionalized iron oxide nanoparticles. Biosensors and Bioelectronics, 2011, 26, 3044-3049.	5.3	36
262	Ultrasensitive electrochemiluminescence immunosensor based on Ru(bpy)32+ and Ag nanoparticles doped SBA-15 for detection of cancer antigen 15-3. Sensors and Actuators B: Chemical, 2013, 188, 462-468.	4.0	36
263	Electrochemiluminescence immunosensing strategy based on the use of Au@Ag nanorods as a peroxidase mimic and NH4CoPO4 as a supercapacitive supporter: Application to the determination of carcinoembryonic antigen. Mikrochimica Acta, 2015, 182, 1421-1429.	2.5	36
264	Sulfur Incorporated CoFe2O4/Multiwalled Carbon Nanotubes toward Enhanced Oxygen Evolution Reaction. Electrochimica Acta, 2017, 247, 843-850.	2.6	36
265	A ternary quenching electrochemiluminescence insulin immunosensor based on Mn2+ released from MnO2@Carbon core-shell nanospheres with ascorbic acid quenching AuPdPt–MoS2@TiO2 enhanced luminol. Biosensors and Bioelectronics, 2019, 142, 111551.	5.3	36
266	MOF-Based Supramolecule Helical Nanomaterials: Toward Highly Enantioselective Electrochemical Recognition of Penicillamine. ACS Applied Materials & Interfaces, 2020, 12, 1533-1538.	4.0	36
267	Polydopamine-PEG–Folic Acid Conjugate Film Engineered TiO ₂ Nanotube Arrays for Photoelectrochemical Sensing of Folate Binding Protein. ACS Applied Materials & Interfaces, 2020, 12, 1877-1884.	4.0	36
268	Triple Amplification of 3,4,9,10-Perylenetetracarboxylic Acid by Co ²⁺ -Based Metal–Organic Frameworks and Silver–Cysteine and Its Potential Application for Ultrasensitive Assay of Procalcitonin. ACS Applied Materials & Interfaces, 2020, 12, 9098-9106.	4.0	36
269	A label-free voltammetric immunoassay based on 3D-structured rGO–MWCNT–Pd for detection of human immunoglobulin G. Sensors and Actuators B: Chemical, 2015, 211, 170-176.	4.0	35
270	Ultrasensitive sandwich-type electrochemical immunosensor based on a novel signal amplification strategy using highly loaded palladium nanoparticles/carbon decorated magnetic microspheres as signal labels. Biosensors and Bioelectronics, 2015, 68, 757-762.	5.3	35

QIN WEI

#	Article	IF	CITATIONS
271	A competitive photoelectrochemical assay for estradiol based on in situ generated CdS-enhanced TiO2. Biosensors and Bioelectronics, 2015, 66, 596-602.	5.3	35
272	A label-free electrochemiluminescence immunosensor based on EuPO4 nanowire for the ultrasensitive detection of Prostate specific antigen. Biosensors and Bioelectronics, 2016, 80, 352-358.	5.3	35
273	Metal–Organic Framework-Derived Co ₃ O ₄ /Au Heterostructure as a Catalyst for Efficient Oxygen Reduction. ACS Applied Materials & Interfaces, 2018, 10, 34068-34076.	4.0	35
274	Anchoring Au(111) on a Bismuth Sulfide Nanorod: Boosting the Artificial Electrocatalytic Nitrogen Reduction Reaction under Ambient Conditions. ACS Applied Materials & Interfaces, 2020, 12, 55838-55843.	4.0	35
275	Label-free electrochemical immunosensor with palladium nanoparticles functionalized MoS2/NiCo heterostructures for sensitive procalcitonin detection. Sensors and Actuators B: Chemical, 2020, 312, 127980.	4.0	35
276	A novel multi-amplification photoelectrochemical immunoassay based on copper(II) enhanced polythiophene sensitized graphitic carbon nitride nanosheet. Biosensors and Bioelectronics, 2014, 62, 315-319.	5.3	34
277	Electrochemiluminescent Immune-Modified Electrodes Based on Ag ₂ Se@CdSe Nanoneedles Loaded with Polypyrrole Intercalated Graphene for Detection of CA72-4. ACS Applied Materials & Interfaces, 2015, 7, 867-872.	4.0	34
278	Simple synthesis of silver nanoparticles functionalized cuprous oxide nanowires nanocomposites and its application in electrochemical immunosensor. Sensors and Actuators B: Chemical, 2016, 236, 241-248.	4.0	34
279	Facile preparation of water-soluble hyperbranched polyamine functionalized multiwalled carbon nanotubes for high-efficiency organic dye removal from aqueous solution. Scientific Reports, 2017, 7, 3611.	1.6	34
280	A novel sandwich-type photoelectrochemical immunosensor based on Ru(bpy)32+ and Ce-CdS co-sensitized hierarchical ZnO matrix and dual-inhibited polystyrene@CuS-Ab2 composites. Biosensors and Bioelectronics, 2019, 129, 124-131.	5.3	34
281	An amplification label of core–shell CdSe@CdS QD sensitized GO for a signal-on photoelectrochemical immunosensor for amyloid β-protein. Journal of Materials Chemistry B, 2019, 7, 1142-1148.	2.9	34
282	Label-free photoelectrochemical immunosensor for amyloid β-protein detection based on SnO2/CdCO3/CdS synthesized by one-pot method. Biosensors and Bioelectronics, 2019, 126, 23-29.	5.3	34
283	A self-powered photoanode-supported photoelectrochemical immunosensor for CYFRA 21-1 detection based on In2O3/In2S3/CdIn2S4 heterojunction. Biosensors and Bioelectronics, 2020, 169, 112580.	5.3	34
284	Preparation of PbS NPs/RGO/NiO nanosheet arrays heterostructure: Function-switchable self-powered photoelectrochemical biosensor for H2O2 and glucose monitoring. Biosensors and Bioelectronics, 2021, 173, 112803.	5.3	34
285	Ultrasensitive enzyme-free immunoassay for squamous cell carcinoma antigen using carbon supported Pd–Au as electrocatalytic labels. Analytica Chimica Acta, 2014, 833, 9-14.	2.6	33
286	Electrochemical aptasensor for the detection of adenosine by using PdCu@MWCNTs-supported bienzymes as labels. Biosensors and Bioelectronics, 2015, 74, 391-397.	5.3	33
287	Responses of soluble microbial products and extracellular polymeric substances to the presence of toxic 2,6-dichlorophenol in aerobic granular sludge system. Journal of Environmental Management, 2016, 183, 594-600.	3.8	33
288	Qualitative and quantitative analysis of extracellular polymeric substances in partial nitrification and full nitrification reactors. Bioresource Technology, 2017, 240, 171-176.	4.8	33

QIN WEI

#	Article	IF	CITATIONS
289	An ultrasensitive electrochemical immunosensor for the detection of prostate-specific antigen based on conductivity nanocomposite with halloysite nanotubes. Analytical and Bioanalytical Chemistry, 2017, 409, 3245-3251.	1.9	33
290	A pH Indicator-linked Immunosorbent assay following direct amplification strategy for colorimetric detection of protein biomarkers. Biosensors and Bioelectronics, 2017, 90, 1-5.	5.3	33
291	Highly-sensitive electrochemiluminescence biosensor for NT-proBNP using MoS2@Cu2S as signal-enhancer and multinary nanocrystals loaded in mesoporous UiO-66-NH2 as novel luminophore. Sensors and Actuators B: Chemical, 2020, 307, 127619.	4.0	33
292	A signal amplification of p DNA@Ag2S based photoelectrochemical competitive sensor for the sensitive detection of OTA in microfluidic devices. Biosensors and Bioelectronics, 2020, 168, 112503.	5.3	33
293	Comparison of nitrous oxide emissions in partial nitrifying and full nitrifying granular sludge reactors treating ammonium-rich wastewater. Bioresource Technology, 2014, 171, 487-490.	4.8	32
294	Sandwich-type amperometric immunosensor using functionalized magnetic graphene loaded gold and silver core-shell nanocomposites for the detection of Carcinoembryonic antigen. Journal of Electroanalytical Chemistry, 2017, 795, 1-9.	1.9	32
295	Novel electrochemical immunosensor for sensitive monitoring of cardiac troponin I using antigen–response cargo released from mesoporous Fe3O4. Biosensors and Bioelectronics, 2019, 143, 111608.	5.3	32
296	Aerobic granular sludge-derived activated carbon: mineral acid modification and superior dye adsorption capacity. RSC Advances, 2015, 5, 25279-25286.	1.7	31
297	A novel electrochemical immunosensor using β-cyclodextrins functionalized silver supported adamantine-modified glucose oxidase as labels for ultrasensitive detection of alpha-fetoprotein. Analytica Chimica Acta, 2015, 893, 49-56.	2.6	31
298	A network signal amplification strategy of ultrasensitive photoelectrochemical immunosensing carcinoembryonic antigen based on CdSe/melamine network as label. Biosensors and Bioelectronics, 2016, 85, 764-770.	5.3	31
299	Label-free electrochemical immunosensor based on enhanced signal amplification between Au@Pd and CoFe2O4/graphene nanohybrid. Scientific Reports, 2016, 6, 23391.	1.6	31
300	Dual-Signaling Electrochemical Ratiometric Method for Competitive Immunoassay of CYFRA21-1 Based on Urchin-like Fe ₃ O ₄ @PDA-Ag and Ni ₃ Si ₂ O ₅ (OH) ₄ -Au Absorbed Methylene Blue Nanotubes. ACS Applied Materials & Interfaces, 2021, 13, 5795-5802.	4.0	31
301	Ultrasensitive electrochemical immunosensor for quantitative detection of tumor specific growth factor by using Ag@CeO2 nanocomposite as labels. Talanta, 2016, 156-157, 11-17.	2.9	30
302	A turn-on fluorescent sensor for Hg2+ detection based on graphene oxide and DNA aptamers. New Journal of Chemistry, 2018, 42, 11147-11152.	1.4	30
303	Ultrasensitive photoelectrochemical immunosensor based on Cu-doped TiO2 and carbon nitride for detection of carcinoembryonic antigen. Carbon, 2019, 146, 276-283.	5.4	30
304	Dual mode competitive electrochemical immunoassay for B-type natriuretic peptide based on GS/SnO2/polyaniline-Au and ZnCo2O4/N-CNTs. Biosensors and Bioelectronics, 2019, 126, 448-454.	5.3	30
305	Effect of turbidity on micropollutant removal and membrane fouling by MIEX/ultrafiltration hybrid process. Chemosphere, 2019, 216, 488-498.	4.2	30
306	Novel Chemiluminescence Sensor for Thrombin Detection Based on Dual-Aptamer Biorecognition and Mesoporous Silica Encapsulated with Iron Porphyrin. ACS Applied Materials & Interfaces, 2020, 12, 5569-5577.	4.0	30

#	Article	IF	CITATIONS
307	Label-free immunosensor based on Au@Ag2S nanoparticles/magnetic chitosan matrix for sensitive determination of ractopamine. Journal of Electroanalytical Chemistry, 2015, 741, 14-19.	1.9	29
308	A novel magnetic polysaccharide–graphene oxide composite for removal of cationic dyes from aqueous solution. New Journal of Chemistry, 2015, 39, 2908-2916.	1.4	29
309	Electrochemiluminescence modified electrodes based on RuSi@Ru(bpy)32+ loaded with gold functioned nanoporous CO/Co3O4 for detection of mycotoxin deoxynivalenol. Biosensors and Bioelectronics, 2015, 70, 28-33.	5.3	29
310	Preparation of Au–Pt nanostructures by combining top-down with bottom-up strategies and application in label-free electrochemical immunosensor for detection of NMP22. Bioelectrochemistry, 2015, 101, 22-27.	2.4	29
311	In situ Formed Co(TCNQ) ₂ Metalâ€Organic Framework Array as a Highâ€Efficiency Catalyst for Oxygen Evolution Reactions. Chemistry - A European Journal, 2018, 24, 2075-2079.	1.7	29
312	A turn-on fluorescent sensor for highly sensitive mercury(<scp>ii</scp>) detection based on a carbon dot-labeled oligodeoxyribonucleotide and MnO ₂ nanosheets. New Journal of Chemistry, 2018, 42, 1228-1234.	1.4	29
313	One-pot synthesis of Ptâ^'Cu bimetallic nanocrystals with different structures and their enhanced electrocatalytic properties. Nano Research, 2018, 11, 2612-2624.	5.8	29
314	Highly-branched Cu2O as well-ordered co-reaction accelerator for amplifying electrochemiluminescence response of gold nanoclusters and procalcitonin analysis based on protein bioactivity maintenance. Biosensors and Bioelectronics, 2019, 144, 111676.	5.3	29
315	AuCu <i>_x</i> O-Embedded Mesoporous CeO ₂ Nanocomposites as a Signal Probe for Electrochemical Sensitive Detection of Amyloid-Beta Protein. ACS Applied Materials & Interfaces, 2019, 11, 12335-12341.	4.0	29
316	Facile fabrication of visible light photoelectrochemical immunosensor for SCCA detection based on BiOBr/Bi2S3 heterostructures via self-sacrificial synthesis method. Talanta, 2019, 198, 417-423.	2.9	29
317	Intramolecular Coreaction Accelerated Electrochemiluminescence of Polypeptide-Biomineralized Gold Nanoclusters for Targeted Detection of Biomarkers. Analytical Chemistry, 2020, 92, 9179-9187.	3.2	29
318	A microfluidic cathodic photoelectrochemical biosensor chip for the targeted detection of cytokeratin 19 fragments 21-1. Lab on A Chip, 2021, 21, 378-384.	3.1	29
319	Dual-signal sandwich electrochemical immunosensor for amyloid β-protein detection based on Cu–Al2O3-g–C3N4–Pd and UiO-66@PANI-MB. Analytica Chimica Acta, 2019, 1089, 48-55.	2.6	28
320	Co-Doped FeS ₂ with a porous structure for efficient electrocatalytic overall water splitting. New Journal of Chemistry, 2020, 44, 1711-1718.	1.4	28
321	Directly assembled electrochemical sensor by combining self-supported CoN nanoarray platform grown on carbon cloth with molecularly imprinted polymers for the detection of Tylosin. Journal of Hazardous Materials, 2020, 398, 122778.	6.5	28
322	Novel Electron Donor Encapsulation Assay Based on the Split-type Photoelectrochemical Interface. ACS Applied Materials & Interfaces, 2020, 12, 7366-7371.	4.0	28
323	A simple label-free photoelectrochemical immunosensor for highly sensitive detection of aflatoxin B ₁ based on CdS–Fe ₃ O ₄ magnetic nanocomposites. RSC Advances, 2015, 5, 19581-19586.	1.7	27
324	Rapid colorimetric detection of melamine by H2O2–Au nanoparticles. RSC Advances, 2015, 5, 32897-32901.	1.7	27

#	Article	IF	CITATIONS
325	Morphology-dependent electrochemical behavior of 18-facet Cu7S4 nanocrystals based electrochemical sensing platform for hydrogen peroxide and prostate specific antigen. Biosensors and Bioelectronics, 2018, 112, 143-148.	5.3	27
326	Sandwich-type signal-off photoelectrochemical immunosensor based on dual suppression effect of PbS quantum dots/Co3O4 polyhedron as signal amplification for procalcitonin detection. Sensors and Actuators B: Chemical, 2019, 300, 127001.	4.0	27
327	Electrochemiluminescence immunosensor of "signal-off―for β-amyloid detection based on dual metal-organic frameworks. Talanta, 2020, 208, 120376.	2.9	27
328	Zinc and Molybdenum Co-Doped BiVO ₄ Nanoarray for Photoelectrochemical Diethylstilbestrol Analysis Based on the Dual-Competitive System of Manganese Hexacyanoferrate Hydrate Nanocubes. ACS Applied Materials & Interfaces, 2020, 12, 16662-16669.	4.0	27
329	Dual-Mode Sensing Platform Guided by Intramolecular Electrochemiluminescence of a Ruthenium Complex and Cationic <i>N</i> , <i>N</i> Bis(2-(trimethylammonium iodide)propylene) Perylene-3,4,9,10-tetracarboxydiimide for Estradiol Assay. Analytical Chemistry, 2021, 93, 6088-6093.	3.2	27
330	Peptide-Based Biosensor with a Luminescent Copper-Based Metal–Organic Framework as an Electrochemiluminescence Emitter for Trypsin Assay. Analytical Chemistry, 2021, 93, 9704-9710.	3.2	27
331	Interface engineering of Fe3O4@MoS2 Nanocomposites: High efficiency electrocatalytic synthesis of NH3 under mild conditions. Chemical Engineering Journal, 2022, 437, 135417.	6.6	27
332	Enhanced electrochemiluminescence from luminol at carboxyl graphene for detection of α-fetoprotein. Analytical Biochemistry, 2014, 457, 59-64.	1.1	26
333	Facile synthesized highly active BiOI/Zn ₂ GeO ₄ composites for the elimination of endocrine disrupter BPA under visible light irradiation. New Journal of Chemistry, 2015, 39, 3964-3972.	1.4	26
334	3D sandwich-type prostate specific antigen (PSA) immunosensor based on rGO–MWCNT–Pd nanocomposite. New Journal of Chemistry, 2015, 39, 5522-5528.	1.4	26
335	Electrochemiluminescence quenching of luminol by CuS in situ grown on reduced graphene oxide for detection of N-terminal pro-brain natriuretic peptide. Biosensors and Bioelectronics, 2018, 112, 40-47.	5.3	26
336	A novel label-free photoelectrochemical immunosensor based on NCQDs and Bi ₂ S ₃ co-sensitized hierarchical mesoporous SnO ₂ microflowers for detection of NT-proBNP. Journal of Materials Chemistry B, 2018, 6, 7634-7642.	2.9	26
337	Electrochemical aptasensor based on Au@HS-rGO and thymine-Hg2+-thymine structure for sensitive detection of mercury ion. Journal of Electroanalytical Chemistry, 2019, 848, 113308.	1.9	26
338	Enhanced electrochemiluminescence of luminol based on Cu2O–Au heterostructure enabled multiple-amplification strategy. Biosensors and Bioelectronics, 2020, 151, 111970.	5.3	26
339	Etching Triangular Silver Nanoparticles by Self-generated Hydrogen Peroxide to Initiate the Response of an Electrochemiluminescence Sensing Platform. Analytical Chemistry, 2020, 92, 14203-14209.	3.2	26
340	Near-Infrared Electrochemiluminescence of Dual-Stabilizer-Capped Au Nanoclusters for Immunoassays. ACS Applied Nano Materials, 2021, 4, 2657-2663.	2.4	26
341	Cysteine Modification of Glutathione-Stabilized Au Nanoclusters to Red-Shift and Enhance the Electrochemiluminescence for Sensitive Bioanalysis. Analytical Chemistry, 2022, 94, 2313-2320.	3.2	26
342	Biomimetic nanopore for sensitive and selective detection of Hg(<scp>ii</scp>) in conjunction with single-walled carbon nanotubes. Journal of Materials Chemistry B, 2014, 2, 6371-6377.	2.9	25

#	Article	IF	CITATIONS
343	An ultrasensitive squamous cell carcinoma antigen biosensing platform utilizing double-antibody single-channel amplification strategy. Biosensors and Bioelectronics, 2015, 72, 156-159.	5.3	25
344	A novel controlled release system-based homogeneous immunoassay protocol for SCCA using magnetic mesoporous Fe3O4 as a nanocontainer and aminated polystyrene microspheres as a molecular gate. Biosensors and Bioelectronics, 2015, 66, 141-145.	5.3	25
345	Ultrasensitive sandwich-type prostate specific antigen immunosensor based on Ag overgrowth in Pd nano-octahedrons heterodimers decorated on amino functionalized multiwalled carbon nanotubes. Sensors and Actuators B: Chemical, 2016, 237, 733-739.	4.0	25
346	Metal oxide- and N-codoped carbon nanosheets: facile synthesis derived from MOF nanofibers and their application in oxygen evolution. Chemical Communications, 2018, 54, 264-267.	2.2	25
347	Label-free electrochemiluminescent immunosensor for detection of prostate specific antigen based on mesoporous graphite-like carbon nitride. Talanta, 2018, 188, 729-735.	2.9	25
348	Electrochemical enantioselective recognition penicillamine isomers based on chiral C-dots/MOF hybrid arrays. Journal of Electroanalytical Chemistry, 2019, 846, 113151.	1.9	25
349	Exciton energy transfer-based fluorescent sensor for the detection of Hg2+ through aptamer-programmed self-assembly of QDs. Analytica Chimica Acta, 2019, 1048, 161-167.	2.6	25
350	Mo-doped porous BiVO4/Bi2S3 nanoarray to enhance photoelectrochemical efficiency for quantitative detection of 17β-estradiol. Sensors and Actuators B: Chemical, 2020, 305, 127443.	4.0	25
351	Rational design of bimetallic Rh _{0.6} Ru _{0.4} nanoalloys for enhanced nitrogen reduction electrocatalysis under mild conditions. Journal of Materials Chemistry A, 2021, 9, 259-263.	5.2	25
352	CuO Nanozymes as Multifunctional Signal Labels for Efficiently Quenching the Photocurrent of ZnO/Au/AgSbS ₂ Hybrids and Initiating a Strong Fluorescent Signal in a Dual-Mode Microfluidic Sensing Platform. ACS Sensors, 2022, 7, 1732-1739.	4.0	25
353	Magnetic hydroxypropyl chitosan functionalized graphene oxide as adsorbent for the removal of lead ions from aqueous solution. Desalination and Water Treatment, 2016, 57, 3975-3984.	1.0	24
354	Disposable competitive-type immunoassay for determination of aflatoxin B1 via detection of copper ions released from Cu-apatite. Talanta, 2016, 147, 556-560.	2.9	24
355	Visible-light driven Photoelectrochemical Immunosensor Based on SnS2@mpg-C3N4 for Detection of Prostate Specific Antigen. Scientific Reports, 2017, 7, 4629.	1.6	24
356	Dual-responsive electrochemical immunosensor for detection of insulin based on dual-functional zinc silicate spheres-palladium nanoparticles. Talanta, 2018, 179, 420-425.	2.9	24
357	Aptamer basedÂelectrochemiluminescent thrombin assay using carbon dots anchored onto silver-decorated polydopamine nanospheres. Mikrochimica Acta, 2018, 185, 85.	2.5	24
358	A signal-off type photoelectrochemical immunosensor for the ultrasensitive detection of procalcitonin: Ru(bpy)32+ and Bi2S3 co-sensitized ZnTiO3/TiO2 polyhedra as matrix and dual inhibition by SiO2/PDA-Au. Biosensors and Bioelectronics, 2019, 142, 111513.	5.3	24
359	GO/PEDOT:NaPSS modified cathode as heterogeneous electro-Fenton pretreatment and subsequently aerobic granular sludge biological degradation for dye wastewater treatment. Science of the Total Environment, 2020, 700, 134536.	3.9	24
360	Enhancing Electrochemiluminescence Efficiency through Introducing Atomically Dispersed Ruthenium in Nickel-Based Metal–Organic Frameworks. Analytical Chemistry, 2022, 94, 10557-10566.	3.2	24

#	Article	IF	CITATIONS
361	A competitive photoelectrochemical immunosensor based on a CdS-induced signal amplification strategy for the ultrasensitive detection of dexamethasone. Scientific Reports, 2015, 5, 17945.	1.6	23
362	CdSe quantum dot-functionalized TiO 2 nanohybrids as a visible light induced photoelectrochemical platform for the detection of proprotein convertase subtilisin/kexin type 6. Biosensors and Bioelectronics, 2015, 71, 88-97.	5.3	23
363	A chemiluminescence aptasensor for thrombin detection based on aptamer-conjugated and hemin/G-quadruplex DNAzyme signal-amplified carbon fiber composite. Analytica Chimica Acta, 2018, 1043, 132-141.	2.6	23
364	Construction of well-ordered electrochemiluminescence sensing interface using peptide-based specific antibody immobilizer and N-(aminobutyl)-N-(ethylisoluminol) functionalized ferritin as signal indicator for procalcitonin analysis. Biosensors and Bioelectronics, 2019, 142, 111562.	5.3	23
365	Construction of the FRET Pairs for the Visualization of Mitochondria Membrane Potential in Dual Emission Colors. Analytical Chemistry, 2019, 91, 3704-3709.	3.2	23
366	A novel ultrasensitive sandwich-type photoelectrochemical immunoassay for PSA detection based on dual inhibition effect of Au/MWCNTs nanohybrids on N-GQDs/CdS QDs dual sensitized urchin-like TiO2. Electrochimica Acta, 2020, 333, 135480.	2.6	23
367	Separation of Biological Events from the Photoanode: Toward the Ferricyanide-Mediated Redox Cyclic Photoelectrochemical System of an Integrated Photoanode and Photocathode. ACS Sensors, 2020, 5, 3540-3546.	4.0	23
368	Fabrication of N-GQDs and AgBiS2 dual-sensitized ZIFs-derived hollow ZnxCo3xO4 dodecahedron for sensitive photoelectrochemical aptasensing of ampicillin. Sensors and Actuators B: Chemical, 2020, 320, 128387.	4.0	23
369	Electrochemiluminescence sensing platform based on functionalized poly-(styrene-co-maleicanhydride) nanocrystals and iron doped hydroxyapatite for CYFRA 21-1 immunoassay. Sensors and Actuators B: Chemical, 2020, 321, 128454.	4.0	23
370	Peptide-Based Electrochemiluminescence Biosensors Using Silver Nanoclusters as Signal Probes and Pd-Cu ₂ 0 Hybrid Nanoconcaves as Coreactant Promoters for Immunoassays. Analytical Chemistry, 2021, 93, 13045-13053.	3.2	23
371	PEGylation Improved Electrochemiluminescence Supramolecular Assembly of Iridium(III) Complexes in Apoferritin for Immunoassays Using 2D/2D MXene/TiO ₂ Hybrids as Signal Amplifiers. Analytical Chemistry, 2021, 93, 16906-16914.	3.2	23
372	Ultrasensitive dual amplification sandwich immunosensor for breast cancer susceptibility gene based on sheet materials. Analyst, The, 2014, 139, 3061-3068.	1.7	22
373	A label-free amperometric immunosensor for the detection of carcinoembryonic antigen based on novel magnetic carbon and gold nanocomposites. RSC Advances, 2015, 5, 19961-19969.	1.7	22
374	Electrochemiluminescence sensor based on cationic polythiophene derivative and NH ₂ –graphene for dopamine detection. RSC Advances, 2015, 5, 5432-5437.	1.7	22
375	Photoelectrochemical determination of Hg(II) via dual signal amplification involving SPR enhancement and a folding-based DNA probe. Mikrochimica Acta, 2017, 184, 1379-1387.	2.5	22
376	Dual-quenching electrochemiluminescence resonance energy transfer system from Ru–In2S3 to α-MoO3-Au based on protect of protein bioactivity for procalcitonin detection. Biosensors and Bioelectronics, 2019, 142, 111524.	5.3	22
377	An ultrasensitive label-free photoelectrochemical sensor based on Ag ₂ O-sensitized WO ₃ /TiO ₂ acicular composite for AFB1 detection. Analytical Methods, 2019, 11, 3890-3897.	1.3	22
378	MoSe ₂ /CdSe Heterojunction Destruction by Cation Exchange for Photoelectrochemical Immunoassays with a Controlled-Release Strategy. Analytical Chemistry, 2021, 93, 10712-10718.	3.2	22

QIN WEI

#	Article	IF	CITATIONS
379	A photoelectrochemical self-powered sensor for the detection of sarcosine based on NiO NSs/PbS/Au NPs as photocathodic material. Journal of Hazardous Materials, 2021, 416, 126201.	6.5	22
380	Hollow Double-Shell CuCo ₂ O ₄ @Cu ₂ O Heterostructures as a Highly Efficient Coreaction Accelerator for Amplifying NIR Electrochemiluminescence of Gold Nanoclusters in Immunoassay. Analytical Chemistry, 2022, 94, 7132-7139.	3.2	22
381	Biosorption of effluent organic matter onto magnetic biochar composite: Behavior of fluorescent components and their binding properties. Bioresource Technology, 2016, 214, 259-265.	4.8	21
382	Copper doped terbium metal organic framework as emitter for sensitive electrochemiluminescence detection of CYFRA 21-1. Talanta, 2022, 238, 123047.	2.9	21
383	Self-powered Aptasensors Made with the In ₂ –Ti ₃ 32 Composite for Dual-mode Detection of Microcystin-LR. ACS Applied Materials & Interfaces, 2022, 14, 25308-25316.	4.0	21
384	Sandwich-type electrochemical immunosensor for ultrasensitive detection of prostate-specific antigen using palladium-doped cuprous oxide nanoparticles. RSC Advances, 2016, 6, 84698-84704.	1.7	20
385	An ultrasensitive label-free electrochemical immunosensor based on signal amplification strategy of multifunctional magnetic graphene loaded with cadmium ions. Scientific Reports, 2016, 6, 21281.	1.6	20
386	An electrochemiluminescence immunosensor for the N-terminal brain natriuretic peptide based on the high quenching ability of polydopamine. Mikrochimica Acta, 2019, 186, 606.	2.5	20
387	Label-free electrochemiluminescent immunosensor for prostate specific antigen ultrasensitive detection based on novel luminophore Ag3PO4 decorated GO. Journal of Electroanalytical Chemistry, 2019, 847, 113266.	1.9	20
388	Ultrasensitive label-free photoelectrochemical immunosensor for the detection of amyloid β-protein based on Zn:SnO2/SnS2-Au nanocomposites. Sensors and Actuators B: Chemical, 2020, 308, 127576.	4.0	20
389	Electrochemiluminescence behaviour of silver/ZnIn2S4/reduced graphene oxide composites quenched by Au@SiO2 nanoparticles for ultrasensitive insulin detection. Biosensors and Bioelectronics, 2020, 162, 112235.	5.3	20
390	Cardiac troponin I photoelectrochemical sensor: {Mo368} as electrode donor for Bi2S3 and Au co-sensitized FeOOH composite. Biosensors and Bioelectronics, 2020, 157, 112157.	5.3	20
391	An ultrasensitive electrochemical immunosensor for determination of estradiol using coralloid Cu ₂ S nanostructures as labels. RSC Advances, 2015, 5, 6512-6517.	1.7	19
392	A robust electrochemiluminescence immunoassay for carcinoembryonic antigen detection based on a microtiter plate as a bridge and Au@Pd nanorods as a peroxidase mimic. Analyst, The, 2016, 141, 337-345.	1.7	19
393	Novel gold nanocluster electrochemiluminescence immunosensors based on nanoporous NiGd–Ni2O3–Gd2O3 alloys. Biosensors and Bioelectronics, 2016, 75, 142-147.	5.3	19
394	Electrochemiluminescence immunoassay for the N-terminal pro-B-type natriuretic peptide based on resonance energy transfer between aÂself-enhanced luminophore composed of silver nanocubes on gold nanoparticles and aÂmetal-organic framework of typeÂMIL-125. Mikrochimica Acta, 2019, 186, 811.	2.5	19
395	Electrochemiluminescence behaviour of silver/silver orthophosphate/graphene oxide quenched by Pd@Au core-shell nanoflowers for ultrasensitive detection of insulin. Biosensors and Bioelectronics, 2020, 147, 111767.	5.3	19
396	Ultrasensitive photoelectrochemical immunosensor for procalcitonin detection with porous nanoarray BiVO4/CuxS platform as advanced signal amplification under anodic bias. Sensors and Actuators B: Chemical, 2020, 308, 127685.	4.0	19

#	Article	IF	CITATIONS
397	A photoelectrochemical immunosensor based on CdS/CdTe-cosensitized SnO ₂ as a platform for the ultrasensitive detection of amyloid \hat{I}^2 -protein. Analyst, The, 2020, 145, 619-625.	1.7	19
398	Antigen down format photoelectrochemical analysis supported by fullerene functionalized Sn ₃ O ₄ . Chemical Communications, 2020, 56, 7455-7458.	2.2	19
399	Artificial N ₂ fixation to NH ₃ by electrocatalytic Ru NPs at low overpotential. Nanotechnology, 2020, 31, 29LT01.	1.3	19
400	In situ evolution of surface Co2CrO4 to CoOOH/CrOOH by electrochemical method: Toward boosting electrocatalytic water oxidation. Chinese Journal of Catalysis, 2021, 42, 1096-1101.	6.9	19
401	A sandwiched photoelectrochemical biosensing platform for detecting Cytokeratin-19 fragments based on Ag2S-sensitized BiOI/Bi2S3 heterostructure amplified by sulfur and nitrogen co-doped carbon quantum dots. Biosensors and Bioelectronics, 2022, 196, 113703.	5.3	19
402	Assembly of graphene nanocomposites into honeycomb-structured macroporous films with enhanced hydrophobicity. New Journal of Chemistry, 2013, 37, 1307.	1.4	18
403	Simultaneous electrochemical immunosensor based on water-soluble polythiophene derivative and functionalized magnetic material. Analytica Chimica Acta, 2014, 845, 85-91.	2.6	18
404	Response of extracellular polymeric substances to the toxicity of 2,4-dichlorophenol in aerobic granular sludge system: production and interaction mechanism. RSC Advances, 2015, 5, 33016-33022.	1.7	18
405	Bare conical nanopore embedded in polymer membrane for Cr(III) sensing. Talanta, 2015, 140, 219-225.	2.9	18
406	A sandwich-type electrochemical immunosensor based on the biotin- streptavidin-biotin structure for detection of human immunoglobulin G. Scientific Reports, 2016, 6, 22694.	1.6	18
407	Label-free electrochemiluminescence immunosensor based on Ce-MOF@g-C3N4/Au nanocomposite for detection of N-terminal pro-B-type natriuretic peptide. Journal of Electroanalytical Chemistry, 2019, 847, 113222.	1.9	18
408	Bifunctional pd-decorated polysulfide nanoparticle of Co9S8 supported on graphene oxide: A new and efficient label-free immunosensor for amyloid β-protein detection. Sensors and Actuators B: Chemical, 2020, 304, 127413.	4.0	18
409	A dual-signal amplification photoelectrochemical immunosensor for ultrasensitive detection of CYFRA 21-1 based on the synergistic effect of SnS2/SnS/Bi2S3 and ZnCdS@NPC-ZnO. Sensors and Actuators B: Chemical, 2021, 346, 130456.	4.0	18
410	A Fluorescence Approach to Assess the Production of Soluble Microbial Products from Aerobic Granular Sludge Under the Stress of 2,4-Dichlorophenol. Scientific Reports, 2016, 6, 24444.	1.6	17
411	A Novel Controlled Release Immunosensor based on Benzimidazole Functionalized SiO2 and Cyclodextrin Functionalized Gold. Scientific Reports, 2016, 6, 19797.	1.6	17
412	Synchronously Achieving Highly Efficient Hydrogen Evolution and High-Yield Synthesis of Glucaric Acid by MOF Nanorod Arrays. Journal of the Electrochemical Society, 2019, 166, H534-H540.	1.3	17
413	Magnetic electrode-based electrochemical immunosensor using amorphous bimetallic sulfides of CoSnSx as signal amplifier for the NT pro BNP detection. Biosensors and Bioelectronics, 2019, 131, 250-256.	5.3	17
414	Novel ratiometric electrochemical sensor for no-wash detection of fluorene-9-bisphenol based on combining CoN nanoarrays with molecularly imprinted polymers. Analyst, The, 2020, 145, 3320-3328.	1.7	17

#	Article	IF	CITATIONS
415	A signal-off electrochemical sensing platform based on Fe3S4-Pd and pineal mesoporous bioactive glass for procalcitonin detection. Sensors and Actuators B: Chemical, 2020, 320, 128324.	4.0	17
416	Coupling of nitrifying granular sludge into microbial fuel cell system for wastewater treatment: System performance, electricity production and microbial community shift. Bioresource Technology, 2021, 326, 124741.	4.8	17
417	Detection of NSE by a photoelectrochemical self-powered immunosensor integrating RGO photocathode and WO3/Mn:CdS nanomaterial photoanode. Biosensors and Bioelectronics, 2022, 207, 114196.	5.3	17
418	Electrochemical Immunosensor for Ultrasensitive Detection of Human Chorionic Gonadotropin Based on Pd@SBAâ€15. Electroanalysis, 2013, 25, 427-432.	1.5	16
419	A biomimetic mussel-inspired photoelectrochemical biosensing chip for the sensitive detection of CD146. Analyst, The, 2015, 140, 5019-5022.	1.7	16
420	Enhanced sensing performance of supported graphitic carbon nitride nanosheets and the fabrication of electrochemiluminescent biosensors for IgG. Analyst, The, 2015, 140, 8172-8176.	1.7	16
421	A novel label-free electrochemical immunosensor for the detection of hepatitis B surface antigen. Analytical Methods, 2016, 8, 7380-7386.	1.3	16
422	An optionality further amplification of an sandwich-type electrochemical immunosensor based on biotin–streptavidin–biotin strategy for detection of alpha fetoprotein. RSC Advances, 2016, 6, 24373-24380.	1.7	16
423	Electrochemiluminescence assay of Cu ²⁺ by using one-step electrodeposition synthesized CdS/ZnS quantum dots. Analyst, The, 2017, 142, 3272-3277.	1.7	16
424	A novel sandwich-type photoelectrochemical sensor for SCCA detection based on Ag ₂ S-sensitized BiOI matrix and Au _{core} Pd _{shell} nanoflower label for signal amplification. New Journal of Chemistry, 2018, 42, 15762-15769.	1.4	16
425	Formation of Homogeneous Epinephrine-Melanin Solutions to Fabricate Electrodes for Enhanced Photoelectrochemical Biosensing. Langmuir, 2018, 34, 7744-7750.	1.6	16
426	A Label-Free Photoelectrochemical Aptasensor Based on N-GQDs Sensitized Zn-SnS ₂ for Aflatoxin B1 Detection. IEEE Sensors Journal, 2019, 19, 1633-1639.	2.4	16
427	Intramolecular Photoelectrochemical System Using Tyrosine-Modified Antibody-Targeted Peptide as Electron Donor for Detection of Biomarkers. Analytical Chemistry, 2020, 92, 10935-10939.	3.2	16
428	Nanoarrays-propped in situ photoelectrochemical system for microRNA detection. Biosensors and Bioelectronics, 2022, 210, 114291.	5.3	16
429	Engineering microstructured porous films for multiple applications via mussel-inspired surface coating. RSC Advances, 2013, 3, 25291.	1.7	15
430	Facile fabrication of an ultrasensitive sandwich-type electrochemical immunosensor for the quantitative detection of alpha fetoprotein using multifunctional mesoporous silica as platform and label for signal amplification. Talanta, 2014, 129, 411-416.	2.9	15
431	Preparation of Au-polydopamine functionalized carbon encapsulated Fe3O4 magnetic nanocomposites and their application for ultrasensitive detection of carcino-embryonic antigen. Scientific Reports, 2016, 6, 21017.	1.6	15
432	Enhanced amperometric immunoassay for the prostate specific antigen using Pt-Cu hierarchical trigonal bipyramid nanoframes asÂa label. Mikrochimica Acta, 2017, 184, 423-429.	2.5	15

#	Article	IF	CITATIONS
433	Ultrasensitive immunoassay of insulin based on highly efficient electrochemiluminescence quenching of carboxyl-functionalized g-C3N4 through coreactant dual-consumption by NiPd-DNAzyme. Journal of Electroanalytical Chemistry, 2018, 818, 168-175.	1.9	15
434	Preparation and characterization of 0D Au NPs@3D BiOI nanoflower/2D NiO nanosheet array heterostructures and their application as a self-powered photoelectrochemical biosensing platform. Nanoscale Advances, 2019, 1, 4313-4320.	2.2	15
435	Copper-Based Metal–Organic Frameworks Loaded with Silver Nanoparticles as Electrochemical Immunosensors for Diethylstilbestrol. ACS Applied Nano Materials, 2019, 2, 8043-8050.	2.4	15
436	Bifunctional peptide-biomineralized gold nanoclusters as electrochemiluminescence probe for optimizing sensing interface. Sensors and Actuators B: Chemical, 2020, 318, 128278.	4.0	15
437	Enzyme-free colorimetric immunoassay for procalcitonin based on MgFe2O4 sacrificial probe with the Prussian blue production. Sensors and Actuators B: Chemical, 2020, 316, 128163.	4.0	15
438	Molecular imprinted photoelectrochemical sensor for bisphenol A supported by flower-like AgBiS2/In2S3 matrix. Sensors and Actuators B: Chemical, 2021, 330, 129387.	4.0	15
439	A duple nanozyme stimulating tandem catalysis assisted multiple signal inhibition strategy for photoelectrochemical bioanalysis. Sensors and Actuators B: Chemical, 2021, 334, 129608.	4.0	15
440	Highly selective electrochemiluminescence aptasensor coupled with mesoporous Fe3O4@Cu@Cu2O as co-reaction accelerator for ATP assay based on target-triggered emitter release. Sensors and Actuators B: Chemical, 2021, 346, 130581.	4.0	15
441	Interface engineering of MoS2@Fe(OH)3 nanoarray heterostucture: Electrodeposition of MoS2@Fe(OH)3 as N2 and H+ channels for artificial NH3 synthesis under mild conditions. Journal of Colloid and Interface Science, 2022, 606, 1374-1379.	5.0	15
442	The Effect of Carbon Nanotubes added into Bullfrog Collagen Hydrogel on Gentamicin Sulphate Release: In Vitro. Journal of Inorganic and Organometallic Polymers and Materials, 2011, 21, 890-892.	1.9	14
443	Assembly of Polyoxometalate-Based Composite Materials. Journal of Inorganic and Organometallic Polymers and Materials, 2012, 22, 301-306.	1.9	14
444	Enzyme-Free Colorimetric Immunoassay for Protein Biomarker Enabled by Loading and Disassembly Behaviors of Polydopamine Nanoparticles. ACS Applied Bio Materials, 2020, 3, 8841-8848.	2.3	14
445	Electrochemiluminescence immunosensor based on ferrocene functionalized ZIF-8 quenching the electrochemiluminescence of Ru(bpy)32+-doped silica nanoparticles embodied N-butyl diethanolamine. Sensors and Actuators B: Chemical, 2021, 329, 129101.	4.0	14
446	Modulating the 0D/2D Interface of Hybrid Semiconductors for Enhanced Photoelectrochemical Performances. Small Methods, 2021, 5, e2100109.	4.6	14
447	Facile Encapsulation of Iridium(III) Complexes in Apoferritin Nanocages as Promising Electrochemiluminescence Nanodots for Immunoassays. Analytical Chemistry, 2021, 93, 11329-11336.	3.2	14
448	Microfluidic Ratiometric Photoelectrochemical Biosensor Using a Magnetic Field on a Photochromic Composite Platform: A Proof-of-Concept Study for Magnetic-Photoelectrochemical Bioanalysis. Analytical Chemistry, 2021, 93, 13680-13686.	3.2	14
449	Photoelectrochemical aptasensor based on La2Ti2O7/Sb2S3 and V2O5 for effectively signal change strategy for cancer marker detection. Biosensors and Bioelectronics, 2021, 192, 113528.	5.3	14
450	Chromium doping: A new approach to regulate electronic structure of cobalt carbonate hydroxide for oxygen evolution improvement. Journal of Colloid and Interface Science, 2022, 609, 414-422.	5.0	14

#	Article	IF	CITATIONS
451	Self-powered photoelectrochemical biosensor with inherent potential for charge carriers drive. Biosensors and Bioelectronics, 2022, 211, 114361.	5.3	14
452	A hierarchical CoMoO ₄ @CoFe-LDH heterostructure as a highly effective catalyst to boost electrocatalytic water oxidation. Dalton Transactions, 2022, 51, 10552-10557.	1.6	14
453	Corrosion inhibition and mechanism of mild steel in hydrochloric acid by ceftriaxone and amoxicillin. Science China Chemistry, 2011, 54, 1529-1536.	4.2	13
454	Photoelectrochemical detection of Cd ²⁺ based on in situ electrodeposition of CdS on ZnO nanorods. Analytical Methods, 2015, 7, 5406-5411.	1.3	13
455	An ultrasensitive electrochemical immunosensor for the detection of CD146 based on TiO ₂ colloidal sphere laden Au/Pd nanoparticles. Analyst, The, 2015, 140, 3557-3564.	1.7	13
456	Removal of basic dyes (malachite green) from aqueous medium by adsorption onto amino functionalized graphenes in batch mode. Desalination and Water Treatment, 2015, 53, 818-825.	1.0	13
457	Sensitive Electrochemical Immunosensor for Detection of Nuclear Matrix Protein-22 based on NH2-SAPO-34 Supported Pd/Co Nanoparticles. Scientific Reports, 2016, 6, 24551.	1.6	13
458	Ru(bpy)32+/nanoporous silver-based electrochemiluminescence immunosensor for alpha fetoprotein enhanced by gold nanoparticles decorated black carbon intercalated reduced graphene oxide. Scientific Reports, 2016, 6, 20348.	1.6	13
459	Hollow Polyhedral Arrays Composed of a Co ₃ O ₄ Nanocrystal Ensemble on a Honeycomb-like Carbon Hybrid for Boosting Highly Active and Stable Evolution Oxygen. Inorganic Chemistry, 2019, 58, 3683-3689.	1.9	13
460	Using PbS–Au heterodimers as signal quencher for the sensitive photoelectrochemical immunoassay of amyloid β-protein. Analytica Chimica Acta, 2019, 1092, 85-92.	2.6	13
461	Mo2C combined with carbon material nanosphere as an electrochemiluminescence super-enhancer and antibody label for ultrasensitive detection of cardiac troponin I. Biosensors and Bioelectronics, 2020, 150, 111910.	5.3	13
462	A cardiac troponin I photoelectrochemical immunosensor: nitrogen-doped carbon quantum dots–bismuth oxyiodide–flower-like SnO2. Mikrochimica Acta, 2020, 187, 332.	2.5	13
463	Electrochemiluminescence detection for β-amyloid1-42 oligomers using silver nanoparticle decorated CuS@CoS2 double shelled nanoboxes as dual-quencher. Sensors and Actuators B: Chemical, 2021, 329, 129155.	4.0	13
464	A sensitive biosensor of CdS sensitized BiVO4/GaON composite for the photoelectrochemical immunoassay of procalcitonin. Sensors and Actuators B: Chemical, 2021, 329, 129244.	4.0	13
465	A dual-mode label-free electrochemical immunosensor for ultrasensitive detection of procalcitonin based on g-C ₃ N ₄ -NiCo ₂ S ₄ -CNTs-Ag NPs. Analyst, The, 2021, 146, 3169-3176.	1.7	13
466	Electrochemiluminescence resonance energy transfer system fabricated by quantum state complexes for cardiac troponin I detection. Sensors and Actuators B: Chemical, 2021, 336, 129733.	4.0	13
467	[Ru(bpy) ₃] ²⁺ @Ce-UiO-66/Mn:Bi ₂ S ₃ Heterojunction and Its Exceptional Photoelectrochemical Aptasensing Properties for Ofloxacin Detection. ACS Applied Bio Materials, 2021, 4, 7186-7194.	2.3	13
468	Ultrasensitive Double-Channel Microfluidic Biosensor-Based Cathodic Photo-electrochemical Analysis via Signal Amplification of SOD-Au@PANI for Cardiac Troponin I Detection. Analytical Chemistry, 2021, 93, 14196-14203.	3.2	13

#	Article	IF	CITATIONS
469	Gold Nanoparticle-Attached Perovskite Cs ₃ Bi ₂ Br ₉ QDs/BiOBr Heterostructures for Photoelectrochemical Biosensing. ACS Applied Nano Materials, 2022, 5, 2812-2819.	2.4	13
470	A photoelectrochemical biosensor for detecting Cytokeratin-19 fragments based on CdS/Ni(OH)2 core-shell nanosphere composites amplified by CdSe@MoSe2. Sensors and Actuators B: Chemical, 2022, 360, 131643.	4.0	13
471	Construction of a photoelectrochemical immunosensor based on CuInS2 photocathode and BiVO4/BiOI/Ag2S photoanode and sensitive detection of NSE. Biosensors and Bioelectronics, 2022, 211, 114368.	5.3	13
472	Addressable Label-Free Photoelectric Sensor Array with Self-Calibration for Detection of Neuron Specific Enolase. Analytical Chemistry, 2022, 94, 6996-7003.	3.2	13
473	Photoelectrochemical immunosensor for the sensitive detection of neuron-specific enolase based on the effect of Z-scheme WO3/NiCo2O4 nanoarrays p-n heterojunction. Biosensors and Bioelectronics, 2022, 213, 114452.	5.3	13
474	Magnetic electrode-based label-free electrochemical impedance spectroscopy immunosensor for sensitive detection of human malignant melanoma markers using gold nanoparticles functionalized magnetic graphene sheets as signal amplifier. RSC Advances, 2014, 4, 59106-59113.	1.7	12
475	Stormwater quality management in rail transportation — Past, present and future. Science of the Total Environment, 2015, 512-513, 353-363.	3.9	12
476	Ultrasensitive electrochemical immunosensor for squamous cell carcinoma antigen detection using lamellar montmorillonite-gold nanostructures as signal amplification. Talanta, 2015, 132, 803-808.	2.9	12
477	An ultrasensitive sandwich-type electrochemical immunosensor for carcino embryonie antigen based on supermolecular labeling strategy. Journal of Electroanalytical Chemistry, 2016, 781, 289-295.	1.9	12
478	Single-step cycle pulse operation of the label-free electrochemiluminescence immunosensor based on branched polypyrrole for carcinoembryonic antigen detection. Scientific Reports, 2016, 6, 24599.	1.6	12
479	Electrochemical procalcitonin immunoassay based on Au@Ag heterojunction nanorods as labels and CeO -CuO nanorods as enhancer. Sensors and Actuators B: Chemical, 2019, 297, 126800.	4.0	12
480	Inner space- and architecture-controlled nanoframes for efficient electro-oxidation of liquid fuels. Journal of Materials Chemistry A, 2019, 7, 19280-19289.	5.2	12
481	Ultrasensitive competitive electrochemiluminescence immunosensor based on luminol-AuNPs@Mo2C and upconversion nanoparticles for detection of diethylstilbestrol. Microchemical Journal, 2020, 158, 105283.	2.3	12
482	Electrochemiluminescence immunosensor based on the quenching effect of CuO@GO on m-CNNS for cTnl detection. Analytical Biochemistry, 2021, 612, 114012.	1.1	12
483	Interface Engineering of CoS ₂ –CeO ₂ /Ti Nanocatalyst for Artificial N ₂ Fixation. ACS Sustainable Chemistry and Engineering, 2021, 9, 13399-13405.	3.2	12
484	Ratiometric Electrochemical Immunosensor Based on L-cysteine Grafted Ferrocene for Detection of Neuron Specific Enolase. Talanta, 2022, 239, 123075.	2.9	12
485	Highly effective visible-photocatalytic hydrogen evolution and simultaneous organic pollutant degradation over an urchin-like oxygen-doped MoS2/ZnIn2S4 composite. Frontiers of Environmental Science and Engineering, 2022, 16, 1.	3.3	12
486	High-Efficiency CdSe Quantum Dots/Fe ₃ O ₄ @MoS ₂ /S ₂ O ₈ ^{2–} Electrochemiluminescence System Based on a Microfluidic Analysis Platform for the Sensitive Detection of Neuron-Specific Enolase. Analytical Chemistry, 2022, 94, 9176-9183.	3.2	12

#	Article	IF	CITATIONS
487	An ultrasensitive sandwich-type electrochemical immunosensor based on Î'-MnO ₂ and palladium nanoparticles covered natural halloysite nanotubes for the detection of hepatitis B surface antigen. New Journal of Chemistry, 2016, 40, 558-563.	1.4	11
488	Electrochemical assay of ampicillin using Fe3N-Co2N nanoarray coated with molecularly imprinted polymer. Mikrochimica Acta, 2020, 187, 442.	2.5	11
489	Recognition of M2 type tumor-associated macrophages with ultrasensitive and biocompatible photoelectrochemical cytosensor based on Ce doped SnO2/SnS2 nano heterostructure. Biosensors and Bioelectronics, 2020, 165, 112367.	5.3	11
490	CoFeOx(OH)y/CoOx(OH)y core/shell structure with amorphous interface as an advanced catalyst for electrocatalytic water splitting. Electrochimica Acta, 2020, 341, 136038.	2.6	11
491	Electrochemiluminescence behaviour of m-CNNS quenched by CeO2@PDA composites for sensitive detection of BNP. Journal of Electroanalytical Chemistry, 2020, 862, 113970.	1.9	11
492	Signal-off electrochemiluminescence immunosensors based on the quenching effect between curcumin-conjugated Au nanoparticles encapsulated in ZIF-8 and CdS-decorated TiO ₂ nanobelts for insulin detection. Analyst, The, 2020, 145, 1858-1864.	1.7	11
493	Direct growth of nickel-doped cobalt phosphide nanowire cluster on carbon cloth for efficient hydrogen evolution reaction. Electrochemistry Communications, 2021, 127, 107051.	2.3	11
494	Competitive electrochemiluminescence aptasensor based on the Ru(II) derivative utilizing intramolecular ECL emission for E2 detection. Sensors and Actuators B: Chemical, 2021, 348, 130717.	4.0	11
495	Electrocatalytic N ₂ Reduction on FeS ₂ Nanoparticles Embedded in Graphene Oxide in Acid and Neutral Conditions. ACS Applied Materials & Interfaces, 2021, 13, 50027-50036.	4.0	11
496	Au modified spindle-shaped cerium phosphate as an efficient co-reaction accelerator to amplify electrochemiluminescence signal of carbon quantum dots for ultrasensitive analysis of aflatoxin B1. Electrochimica Acta, 2022, 407, 139912.	2.6	11
497	Eu(II)-MOF as NIR probe for highly efficient instantaneous anodic electroluminescence realized environmental pollutant trace monitoring. Chemical Engineering Journal, 2022, 446, 136912.	6.6	11
498	Efficient ABEI–Dissolved O ₂ –Ce(III, IV)-MOF Ternary Electrochemiluminescent System Combined with Self-Assembled Microfluidic Chips for Bioanalysis. Analytical Chemistry, 2022, 94, 9363-9371.	3.2	11
499	Dual Direct Z-Scheme Heterojunction with Growing Photoactive Property for Sensitive Photoelectrochemical and Colorimetric Bioanalysis. Analytical Chemistry, 2022, 94, 9888-9893.	3.2	11
500	Achieving Z-scheme charge transfer through constructing Bi4Ti3O12/Pd@Au/Ag2S heterostructure for photoelectrochemical aptasensor of Hg2+ detection. Sensors and Actuators B: Chemical, 2022, 369, 132385.	4.0	11
501	Ultrasensitive label-free immunoassay for diethylstilbestrol based on Au nanoparticles on mesoporous silica and amino-functionalized graphene. Analytical Methods, 2013, 5, 5534.	1.3	10
502	An electrochemiluminescence sensor for bromate assay based on a new cationic polythiophene derivative. Analytica Chimica Acta, 2014, 852, 69-73.	2.6	10
503	Layer-by-layer self-assembly of 2D graphene nanosheets, 3D copper oxide nanoflowers and 0D gold nanoparticles for ultrasensitive electrochemical detection of alpha fetoprotein. RSC Advances, 2015, 5, 56583-56589.	1.7	10
504	An electrochemiluminescent immunosensor based on CdS–Fe ₃ O ₄ nanocomposite electrodes for the detection of Ochratoxin A. New Journal of Chemistry, 2015, 39, 4259-4264.	1.4	10

#	Article	IF	CITATIONS
505	A sensitive photoelectrochemical immunoassay based on mesoporous carbon/core–shell quantum dots as donor–acceptor light-harvesting architectures. New Journal of Chemistry, 2015, 39, 731-738.	1.4	10
506	A comparison of the influence of flocculent and granular structure of sludge on activated carbon: preparation, characterization and application. RSC Advances, 2016, 6, 87353-87361.	1.7	10
507	Novel electrochemiluminescent platform based on gold nanoparticles functionalized Ti doped BiOBr for ultrasensitive immunosensing of NT-proBNP. Sensors and Actuators B: Chemical, 2018, 277, 401-407.	4.0	10
508	Electrochemiluminescent immunoassay for insulin by using a quencher pair consisting of CdS:Eu nanoclusters loaded with multiwalled carbon nanotubes on reduced graphene oxide nanoribbons and gold nanoparticle-loaded octahedral Cu2O. Mikrochimica Acta, 2019, 186, 505.	2.5	10
509	A procalcitonin photoelectrochemical immunosensor: NCQDs and Sb ₂ S ₃ co-sensitized hydrangea-shaped WO ₃ as a matrix through a layer-by-layer assembly. New Journal of Chemistry, 2020, 44, 2452-2458.	1.4	10
510	Signal-off electrochemiluminescence immunosensor based on Mn-Eumelanin coordination nanoparticles quenching PtCo-CuFe2O4-reduced graphene oxide enhanced luminol. Sensors and Actuators B: Chemical, 2020, 323, 128702.	4.0	10
511	THCH as electron donor in controlled-release system for procalcitonin analysis based on Bi2Sn2O7 photoanode. Sensors and Actuators B: Chemical, 2020, 321, 128509.	4.0	10
512	Polyacrylic acid/polyethylene glycol hybrid antifouling interface for photoelectrochemical immunosensing of MDA-MB-231 cells using BiOBr/FeTPPCl/BiOI co-sensitized composite as matrix. Sensors and Actuators B: Chemical, 2021, 328, 129081.	4.0	10
513	Vanadium-doped NiS ₂ porous nanospheres with high selectivity and stability for the electroreduction of nitrogen to ammonia. Inorganic Chemistry Frontiers, 2021, 8, 3266-3272.	3.0	10
514	A dual signal-amplified electrochemiluminescence immunosensor based on core-shell CeO2-Au@Pt nanosphere for procalcitonin detection. Mikrochimica Acta, 2021, 188, 344.	2.5	10
515	Dual-quenching electrochemiluminescence resonance energy transfer system from IRMOF-3 coreaction accelerator enriched nitrogen-doped GQDs to ZnO@Au for sensitive detection of procalcitonin. Sensors and Actuators B: Chemical, 2021, 346, 130495.	4.0	10
516	MoS ₂ â€Based Catalysts for N ₂ Electroreduction to NH ₃ – An Overview of MoS ₂ Optimization Strategies. ChemistryOpen, 2021, 10, 1041-1054.	0.9	10
517	Bioactivity-protective electrochemiluminescence sensor using CeO2/Co4N heterostructures as highly effective coreaction accelerators for ultrasensitive immunodetection. Sensors and Actuators B: Chemical, 2022, 355, 131158.	4.0	10
518	Highly sensitive photoelectrochemical neuron specific enolase analysis based on cerium and silver Co-Doped Sb2WO6. Biosensors and Bioelectronics, 2022, 203, 114047.	5.3	10
519	Ratiometric electrochemical immunoassay for procalcitonin based on dual signal probes: Ag NPs and Nile blue A. Mikrochimica Acta, 2022, 189, 126.	2.5	10
520	Designing Triangular Silver Nanoplates with GSH/GSSG Surface Mixed States as Novel Nanoparticle-based Redox Mediators for Electrochemical Biosensing. ACS Applied Materials & Interfaces, 2022, 14, 26271-26278.	4.0	10
521	Progress and Prospects of Electrochemiluminescence Biosensors Based on Porous Nanomaterials. Biosensors, 2022, 12, 508.	2.3	10
522	A label-free electrochemical immunosensor with a novel signal production and amplification strategy based on three-dimensional pine-like Au–Cu nanodendrites. RSC Advances, 2015, 5, 31262-31269.	1.7	9

#	Article	IF	CITATIONS
523	Comparison of soluble microbial products released from activated sludge and aerobic granular sludge systems in the presence of toxic 2,4-dichlorophenol. Bioprocess and Biosystems Engineering, 2017, 40, 309-318.	1.7	9
524	An electrochemical immunosensor based on a multiple signal amplification strategy for highly sensitive detection of prostate specific antigen. Analytical Methods, 2018, 10, 4917-4925.	1.3	9
525	A novel photoelectrochemical singal amplification assay for procalcitonin detection based on ZnxBi2S3+x sensitized NiTiO3 matrix. Sensors and Actuators B: Chemical, 2019, 301, 127099.	4.0	9
526	Fast and sensitive fluorescent probe for ratiometric detection of hydrogen sulfide in mitochondria. Analytical Methods, 2019, 11, 232-235.	1.3	9
527	Synergy of Cobalt Iron Tetrathiomolybdate Coated on Cobalt Iron Carbonate Hydroxide Hydrate Nanowire Arrays for Overall Water Splitting. ChemElectroChem, 2020, 7, 2309-2313.	1.7	9
528	Label-Free Antifouling Photoelectrochemical Sensing Strategy for Detecting Breast Tumor Cells Based on Ligand–Receptor Interactions. ACS Applied Bio Materials, 2021, 4, 4479-4485.	2.3	9
529	Hollow performances quenching label of Au NPs@CoSnO3 nanoboxes-based sandwich photoelectrochemical immunosensor for sensitive CYFRA 21-1 detection. Talanta, 2021, 233, 122552.	2.9	9
530	Sandwich-type photoelectrochemical immunosensor for procalcitonin detection based on Mn2+ doped CdS sensitized Bi2WO6 and signal amplification of NaYF4:Yb, Tm upconversion nanomaterial. Analytica Chimica Acta, 2021, 1188, 339190.	2.6	9
531	Self-powered photoelectrochemical aptasensor based on MIL-68(In) derived In2O3 hollow nanotubes and Ag doped ZnIn2S4 quantum dots for oxytetracycline detection. Talanta, 2022, 240, 123153.	2.9	9
532	Label-free electrochemical immunosensors for the detection of zeranol using graphene sheets and nickel hexacyanoferrate nanocomposites. Analytical Methods, 2013, 5, 4159.	1.3	8
533	Hydrophobic bifunctionalized hexagonal mesoporous silicas as efficient adsorbents for the removal of Orange IV. RSC Advances, 2014, 4, 49783-49788.	1.7	8
534	Electrochemical behavior of Keggin-type heteropolyanion doped composite of polyaniline and multi-walled carbon nanotubes. Journal of Molecular Liquids, 2015, 206, 335-337.	2.3	8
535	Enhanced photoelectrochemical aptasensing platform for TXNDC5 gene based on exciton energy transfer between NCQDs and TiO2 nanorods. Scientific Reports, 2016, 6, 19202.	1.6	8
536	Electrogenerated Chemiluminescence Behavior of Au nanoparticles-hybridized Pb (II) metal-organic framework and its application in selective sensing hexavalent chromium. Scientific Reports, 2016, 6, 22059.	1.6	8
537	Production of soluble microbial products in aerobic granular sludge system under the stress of toxic 4-chlorophenol. Environmental Technology (United Kingdom), 2017, 38, 3192-3200.	1.2	8
538	Porous Fe–N-codoped carbon microspheres: an efficient and durable electrocatalyst for oxygen reduction reaction. Inorganic Chemistry Frontiers, 2018, 5, 2211-2217.	3.0	8
539	Anchoring CuO Nanoparticles On C, Nâ€Codoped <i>Gâ€</i> C ₃ N ₄ Nanosheets from Melamineâ€Entrapped MOF Gel for Highâ€Efficiency Oxygen Evolution. ChemNanoMat, 2019, 5, 1170-1175.	1.5	8
540	Dual Intramolecular Electron Transfer for In Situ Coreactantâ€Embedded Electrochemiluminescence Microimaging of Membrane Protein. Angewandte Chemie, 2021, 133, 199-203.	1.6	8

#	Article	IF	CITATIONS
541	Split-Type Electrochemical Immunoassay System Triggering Ascorbic Acid-Mediated Signal Magnification Based on a Controlled-Release Strategy. ACS Applied Materials & Interfaces, 2021, 13, 29179-29186.	4.0	8
542	No-wash point-of-care biosensing assay for rapid and sensitive detection of aflatoxin B1. Talanta, 2021, 235, 122772.	2.9	8
543	A Facile Electrochemical Immunosensor with Mesoporous Alumina for Detection of Carcinoembryonic Antigen. Electroanalysis, 2011, 23, 1602-1606.	1.5	7
544	Mulberry-like gold nanospheres supported on graphene nanosheets: one-pot synthesis, characterization and photoelectrochemical property. New Journal of Chemistry, 2014, 38, 3166.	1.4	7
545	An electrochemical immunosensor for ultrasensitive detection of HBsAg based on platinum nanoparticles loaded on natural montmorillonite. Analytical Methods, 2015, 7, 9150-9157.	1.3	7
546	Ternary Pt@Pd@Ru nanodendrite-decorated graphene oxide for sensitive electrochemical immunoassy of CEA. RSC Advances, 2016, 6, 42994-42999.	1.7	7
547	Ternary Pt-Co-Cu nanodendrites for ultrasensitive voltammetric determination of insulin at very low working potential. Mikrochimica Acta, 2017, 184, 2031-2038.	2.5	7
548	A magnetic activated sludge for Cu(<scp>ii</scp>) and Cd(<scp>ii</scp>) removal: adsorption performance and mechanism studies. New Journal of Chemistry, 2019, 43, 18062-18071.	1.4	7
549	A novel molecularly imprinted electrochemiluminescence sensor based on cobalt nitride nanoarray electrode for the sensitive detection of bisphenol S. RSC Advances, 2021, 11, 11011-11019.	1.7	7
550	Sphereâ€onâ€Tube Biomimetic Hierarchical Nanostructures Coupled with Engineered Surfaces for Enhanced Photoelectrochemical Biosensing of Cancer Cells Expressing Folate Receptors. Advanced Materials Interfaces, 2021, 8, 2100421.	1.9	7
551	Ultrasensitive Photochemical Immunosensor Based on Flowerlike SnO2/BiOI/Ag2S Composites for Detection of Procalcitonin. Biosensors, 2021, 11, 421.	2.3	7
552	Spectroscopic studies of aggregation behavior of <i>meso</i> -tetra(4-hydroxyphenyl)porphyrin in aqueous AOT solution. Journal of Porphyrins and Phthalocyanines, 2008, 12, 101-108.	0.4	6
553	Screen Printed Biosensor for Hydrogen Peroxide Based on Prussian Blue Modified Hydroxyapatite. Journal of Inorganic and Organometallic Polymers and Materials, 2013, 23, 917-922.	1.9	6
554	Ultrasensitive electrochemiluminescence immunosensor for detection of ochratoxin A based on gold nanoparticles-hybridized mesoporous carbon. Analytical Methods, 2014, 6, 5766-5770.	1.3	6
555	Synthesis of PtPb hollow nanoparticles and their application in an electrochemical immunosensor as signal tags for detection of dimethyl phthalate. RSC Advances, 2015, 5, 57346-57353.	1.7	6
556	A sensitive electrochemical immunosensor for the detection of squamous cell carcinoma antigen by using PtAu nanoparticles loaded on TiO ₂ colloidal spheres as labels. RSC Advances, 2015, 5, 59853-59860.	1.7	6
557	Signal Amplification Strategy of Triple-Layered Core–Shell Au@Pd@Pt Nanoparticles for Ultrasensitive Immunoassay Detection of Squamous Cell Carcinoma Antigen. Journal of Biomedical Nanotechnology, 2015, 11, 245-252.	0.5	6
558	Application of three-dimensional flower-like nanomaterials in the fabrication of sandwich-type electrochemical immunosensors. RSC Advances, 2015, 5, 88160-88165.	1.7	6

#	Article	IF	CITATIONS
559	Original signal amplification assay for N-Terminal pro-brain natriuretic peptide detection based on Bi2MoO6 photosensitive matrix. Analytica Chimica Acta, 2020, 1101, 58-64.	2.6	6
560	Photoelectrochemical self-powered biosensing cathodic platform by NiO nanosheets/RGO/BiOI heterostructures for detection of glucose. Journal of Electroanalytical Chemistry, 2020, 876, 114497.	1.9	6
561	Spectroscopic Investigation and Nanoscale Characterization of Epinephrine Autooxidation under Alkaline Conditions. Langmuir, 2020, 36, 5040-5047.	1.6	6
562	Liposome encapsulated electron donor strategy for signal-on CYFRA 21-1 photoelectrochemical analysis. Mikrochimica Acta, 2021, 188, 75.	2.5	6
563	Ni foam supported photocathode platform for DNA detection based on antifouling interface. Sensors and Actuators B: Chemical, 2021, 333, 129593.	4.0	6
564	Electrocatalytic excitation and Co-reaction acceleration synergistic amplification signal of hydrazide-conjugated carbon dots for an electrochemiluminescence immunoassay. Sensors and Actuators B: Chemical, 2022, 357, 131443.	4.0	6
565	Cobalt ion doping to improve electrochemiluminescence emisssion of gold nanoclusters for sensitive NIR biosensing. Sensors and Actuators B: Chemical, 2022, 367, 132034.	4.0	6
566	High-efficient biosorption of dye wastewater onto aerobic granular sludge and photocatalytic regeneration of biosorbent by acid TiO2 hydrosol. Environmental Science and Pollution Research, 2018, 25, 27606-27613.	2.7	5
567	A voltammetric immunoassay for the carcinoembryonic antigen using a self-assembled magnetic nanocomposite. Mikrochimica Acta, 2018, 185, 387.	2.5	5
568	A novel approach to photoelectrochemical immunoassay for procalcitonin on the basis of SnS ₂ /CdS. New Journal of Chemistry, 2020, 44, 15281-15288.	1.4	5
569	Rationally engineered high-performance BiVO4/Ag3VO4/SnS2 photoelectrodes for ultrasensitive immunosensing of CYFRA21-1 based on HRP-tyramine-triggered insoluble precipitates. Mikrochimica Acta, 2021, 188, 270.	2.5	5
570	Structural basis and molecular mechanism of biased GPBAR signaling in regulating NSCLC cell growth via YAP activity. Proceedings of the National Academy of Sciences of the United States of America, 2022, 119, .	3.3	5
571	Preparation, Characterization and Adsorption Performance of Cetyl Pyridine Bromide Modified Bentonites. Journal of Inorganic and Organometallic Polymers and Materials, 2012, 22, 42-47.	1.9	4
572	Qualitative and quantitative spectrometric evaluation of soluble microbial products formation in aerobic granular sludge system treating nitrate wastewater. Bioprocess and Biosystems Engineering, 2018, 41, 841-850.	1.7	4
573	A photoelectrochemical aptasensor for the detection of 17β-estradiol based on In ₂ S ₃ and CdS co-sensitized cerium doped TiO ₂ . New Journal of Chemistry, 2020, 44, 346-353.	1.4	4
574	A Noâ€washing Pointâ€ofâ€Care Electrochemical Biosensor Based on CuS Nanoparticles for Rapid and Sensitive Detection of Neuronâ€specific Enolase. Electroanalysis, 2022, 34, 338-344.	1.5	4
575	Design of MOFâ€Đerived NiOâ€Carbon Nanohybrids Photocathodes Sensitized with Quantum Dots for Solar Hydrogen Production. Small, 2022, 18, e2201815.	5.2	4
576	Meso-Tetra-(3,5-Dibromo-4-Hydroxydroxyphenyl) Porphyrin Copper (II) Self-Assembled Modified Gold Electrode Through l-Cysteine: The Preparation, Electrochemical Behavior and its Application. Journal of Inorganic and Organometallic Polymers and Materials, 2011, 21, 871-875.	1.9	3

#	Article	IF	CITATIONS
577	Honeycomb-Structured Porous Films Prepared from Polymer Nanocomposites of Gold Nanorods. Journal of Inorganic and Organometallic Polymers and Materials, 2013, 23, 587-591.	1.9	3
578	Rapid and high-efficiency removal of methylene blue onto low-cost activated sludge: Role and significance of extracellular polymeric substances. Bioresource Technology Reports, 2019, 7, 100240.	1.5	3
579	Anaerobic granular sludge-derived activated carbon: preparation, characterization and superior dye adsorption capacity. Desalination and Water Treatment, 2016, 57, 18016-18027.	1.0	2
580	Fluorescent component and complexation mechanism of extracellular polymeric substances during dye wastewater biotreatment by anaerobic granular sludge. Royal Society Open Science, 2018, 5, 171445.	1.1	2
581	High-performance ammonia fixation electrocatalyzed by ReS ₂ nanosheet array. New Journal of Chemistry, 2021, 45, 11457-11460.	1.4	2
582	Quenching and binding mechanism of the intrinsic fluorescence of bovine serum albumin by 5-phenyl-10,15,20-tri-(4-pyridyl)-porphyrin. Journal of Porphyrins and Phthalocyanines, 2009, 13, 933-938.	0.4	1
583	Self-Aggregation Behavior of <i>meso</i> -Tetra-(4-trimethylaminophenyl)porphyrin Encapsulated in Reverse Micelles. Spectroscopy Letters, 2010, 43, 275-281.	0.5	1
584	Label-free electrochemical immunoassay for ultrasensitive detection of norethindrone. Monatshefte Für Chemie, 2014, 145, 155-160.	0.9	1
585	Nutrient recovery in anaerobic membrane bioreactors. , 2020, , 283-307.		1
586	Cation Decorated Ferric Oxide with a Polyhedralâ€like Structure for the Electrocatalytic Nitrogen Reduction Reaction. ChemCatChem, 2021, 13, 4990-4997.	1.8	1
587	Synergistic enhancement effect of polydopamine–polyethyleneimine hybrid films for a visible-light photoelectrochemical biosensing interface. ChemPhysMater, 2023, 2, 69-76.	1.4	1
588	Self-supported and defect-rich CoP nanowire arrays with abundant catalytic sites as a highly efficient bifunctional electrocatalyst for water splitting. New Journal of Chemistry, 2022, 46, 13117-13121.	1.4	1
589	Determination of Nucleic Acids Sensitized by Emulsifier OPâ€micelle Using Ethyl Rhodamine B as a Resonance Lightâ€Scattering Probe. Spectroscopy Letters, 2007, 40, 627-641.	0.5	0
590	Biological treatment of high strength ammonia wastewater containing 2,4-dichlorophenol in a membrane bioreactor: System performance and microbial community. Bioresource Technology Reports, 2019, 7, 100233.	1.5	0